Investigation of different parameters on the performance of single lap joints

Dissertation submitted in partial fulfillment of the requirement
for the award of degree
of

Master of Engineering
in
CAD/CAM Engineering

Submitted By
JASPREET SINGH
Roll No. 801584011

Under the supervision of

Dr. Jaswinder Singh Saini
Associate Professor
Mechanical Engineering Department

Dr. Haripada Bhunia
Professor
Chemical Engineering Department

MECHANICAL ENGINEERING DEPARTMENT
THAPAR UNIVERSITY
PATIALA-147004, PUNJAB, INDIA
JULY 2017

DECLARATION

This is to certified that dissertation entitled, "**Investigation of different parameters on the performance of single lap joints**", submitted by me in partial fulfilment of the requirements for the award of Masters of Engineering Degree in CAD/CAM Engg. At Thapar University, Patiala is an authentic work carried out by me under the supervision and guidance of Dr. J.S. Saini, Associate Professor, Department of Mechanical Engineering and Dr. Haripada Bhunia, Professor, Department of Chemical Engineering, Thapar University, Patiala.

Jaspreet Singh

Date: 17/07/2017

Jaspreet Singh
Roll No. 801584011

It is certified that the above statement made by the student is correct to the best of our knowledge and belief.

17/7/17

Dr. J.S. Saini
Associate Professor
Department of Mechanical Engineering

17-07-2017

Dr. Haripada Bhunia
Professor
Department of Chemical Engineering

ACKNOWLEDGEMENTS

Through this, I would like to thanks to all the great people who influences me in a positive direction till now. It is all started during my Master's course in Thapar University, when I got familiar with an intellectual personality, **Dr. Jaswinder Singh Saini**, who taught me two major subjects of CAD/CAM Engineering *i.e.*, Finite Element Method and Computer Aided Design. His unique way of teaching with complete calmness inspired me a lot to carry out my research work under his guidance.

Fortunately, after six months of Master's admission, I got the wonderful opportunity to work under his supervision. I would like to acknowledge my guide **Dr. Jaswinder Singh Saini, Associate Professor, Department of Mechanical Engineering, Thapar University, Patiala,** for his beneficial propositions and enthusiastic guidance in the thesis work. I would also like to acknowledge my co-guide **Dr. Haripada Bhunia, Professor, Department of Chemical Engineering, Thapar University, Patiala,** for his valuable suggestions and quality supervision.

Now, I would like to show my deepest gratitude to **Mr. Manjeet Singh** and **Mr. Kulwinder Singh, Research Scholar, Thapar University, Patiala,** who supported me at huge level and making me able to grasp the technical details related to research work. At last, I would like to acknowledge all my friends who always encouraged me throughout my complete research work, especially, **Mr. Kamaldeep Sharma, Mr. Gaganpreet Singh Hunjan, and Mr. Amardeep Singh.**

My parents, who gave me the strength and support behind all my work, which helped me to sustain easily at the most difficult time.

Jaspreet Singh

ABSTRACT

The efficiency of the machines have become key point for competition among automotive and aircraft industries. In order to reduce the fuel consumption and increase the efficiency, industry has a huge focus on development of lightweight materials with the comparative performance to the traditional metals. Fiber reinforced plastics, while being light in weight and having high load bearing capacities are often used in place of traditional sheet metal components in the body shop. In real life applications, different components needs to be joined together to perform the desired function. Mechanical joints generally incur low cost and facilitates easy disassembly for the maintenance without damaging the basic components. Bolt torque, washer and geometry of the joint are the important parameters, which affects the performance of the joint. Therefore, to analyse the effects of aforesaid parameters, the present study deals with experimental and numerical investigations on failure analysis of the single lap single bolt joint under tensile loads. For manufacturing composite laminates, 2D woven glass fiber has been used as reinforcement in the epoxy. Two different levels of torque *i.e.*, 0 Nm and 5 Nm were used to analyse the effect of bolt pretension on the joint performance. To study the effect of washer size on the failure behaviour, outer diameter of the washer was varied from 12 mm to 16 mm. The geometric parameters *i.e.*, w/d and e/d have been varied from 3 to 5 and 3 to 4 respectively. From the experimental results, increasing the initial bolt pretension and w/d ratio has shown increase in the failure load of the joint. However the efficiency of the joint decreases with increase in w/d ratio. It was observed that the stiffness of the bolt joint increases by reducing the outer diameter of the washer. Increasing w/d ratio has shown a positive effect on the joint stiffness. For numerical analysis, characteristic curve method along with Tsai-Wu failure criteria has been used in the ANSYS software. There was a good agreement between the numerical and experimental results.

TABLE OF CONTENT

LIST OF FIGURES

LIST OF TABLES

ABBREVIATIONS

FRC - Fibre Reinforced Composites

ASTM - American Society for Testing and Materials

UTM - Universal Testing Machine

FEA - Finite Element Analysis

CFRP - Carbon Fibre Reinforced Polymer

SEM – Scanning Electron Microscopy

GFRP – Glass Fibre Reinforced Polymer

LIST OF SYMBOLS

A_r- Resisting area

F - Failure load

P - Applied Load

E_1 - Longitudinal Modulus

E_2 - Transverse Modulus

S - Shear strength

X_t - Longitudinal Strength in Tension

Y_t - Transverse Strength in Tension

X_c - Longitudinal Strength in Compression

Y_c - Transverse Strength in Compression

ν_{12} - Poisson Ratio

e - Distance from side edge to centre of the hole

w - Width of the plate

l - Length of the plate

d - Diameter of the hole

D - Outer diameter of washer

t - Thickness of plate

σ_t - Tensile Strength

τ_s - Shearing Strength

σ_b - Bearing Strength

CHAPTER 1

INTRODUCTION

A composite material is formed when two or more constitute having significantly different properties to each other are combined together at macroscopic level. The advantage of composite material is that, they exhibit some of the properties better than constitutes they are made from. In general, there are two constitutes, one is called reinforcement and other one is called matrix. Various types of reinforcements are available to form composite materials, however, fibre reinforcement plays better role in the structural applications. Matrix is a binder material, which holds the fibres or whiskers together to form a structural element that can carry the load. The purpose of matrix is not only to support the fibres or whiskers and to protect them environmentally but also to transfer load. In most of cases matrix has lower density, strength and stiffness than the fibres or whiskers. However, reinforcing fibres into matrix, strength and stiffness can be improved, yet the density is low. Depending upon application matrix material can be metal, ceramics, polymer, glass or carbon. In comparison to traditional materials, composite materials; that have high specific strength and specific modulus, have become important in weight-sensitive applications such as space vehicles and aircrafts [1].

1.1 Classification of Composites

Broadly, on the basis of constitute used in composite materials, it can be categorised into the as follows:

- The first category is described with respect to reinforcement used which comprises of fibrous composite materials, laminated composite materials and particulate composite materials and combination of composite materials. Fibrous reinforced composites are further classified into discontinuous and continuous fibres.
- The second category is described with respect to matrix phase of composite material. It consist of Metal Matrix Composites (MMCs), Ceramic Matrix Composites (CMCs) and Organic Matrix Composites (OMCs). Further, OMC can also be classified into Polymer Matrix Composite (PMCs) and Carbon Matrix Composites.

1.1.1 Fibrous Composite Materials

Fibrous composite materials consist of fibres reinforced into a matrix. Long fibres are much stiffer and stronger than the material in bulk form. This behaviour of fibres is due to its perfect structure and crystal alignment along the fibre axis. Besides of this in the fibres, internal defects are less than that of bulk material of fibres. The geometrical characterization of fibre is not only

by its high aspect ratio but also by its near crystal sized diameter. Whiskers can be differentiated from fibres on the basis of aspect ratio. Aspect ratio of whiskers is less than the length to diameter ratio of fibres but it has the same near crystal sizes diameter as fibre.

1.1.2 Laminated Composite Materials

Laminated composite materials are made up of layers of at least two different materials that are bonded together. In hybrid composite materials these individual layers can be of different materials. Various properties such as strength, stiffness, corrosion resistance, thermal insulation and acoustical insulation etc. can be altered upon lamination of different layers. Stacking sequence of different layers in laminate will decide the coupling between in-plane and out-of-plane stresses. Each layer of laminate can be either orthotropic or transversally isotropic in nature, depends upon the layer orientation in the laminate.

1.1.3 Particulate Composite Materials

Particulate composite materials are formed when the particles of one or more materials are suspended into matrix of another material. The particles used to form composite can be either metallic or non-metallic. On the basis of material of particles, particulate composite can also be further classified as Nano-composites. Reinforcement of particles to the matrix offers several advantages. It not only strengthen the matrix but also increases number of other properties. For example, the reinforcement of conductive particles in the plastic matrix can improve the conductive properties of the plastic matrix.

1.1.4 Combination of Composite Materials

It is the combination of some or all of the above three types. For example, reinforced concrete is the combination of both fibrous and particulate composite materials. Laminated fibre reinforced composite materials are the combination of both laminated and fibrous composite material types.

1.1.5 Polymer Matrix Composite

As it is already discussed composite material is multiphase system in which matrix is continues phase and fibre is a dispersed phase. Although fibre is the main load bearing component of composite material and the strength of fibre is more than that of matrix, matrix transfers the load from one fibre to other fibre. Therefore, the performance of composite material depends upon the performance of both fibre and matrix.

Fibre reinforced plastic is one of the composite materials in which organic polymer is used as matrix material and fibre is used as reinforcement. Due to very good adhesive properties of

polymer, there is very good interfacial bonding between fibre and matrix which leads to excellent mechanical properties of polymer matrix composite material.

1.2 Advantages and disadvantages of polymer matrix laminated composites

Several advantages of polymer composite material overweight the use of it. Following are some of the advantages and disadvantages of polymer matrix laminated composite material.

(i) **Specific strength and stiffness:** For the same weight, composite materials have more strength than the metallic materials. Specific strength and specific stiffness is the ratio of strength to density and stiffness to density, respectively. High specific strength and high specific stiffness is the over weighted advantage of composite material.

(ii) **Fatigue Strength:** Unlike the traditional materials, fatigue strength of composite material is high. Fatigue failure always initiates from the weak areas of structure such as crack or void. But due to progressive damage of composite materials, fatigue strength of composite material is more than the fatigue strength of metal. In general, fatigue strength of metals is 30-50% of its tensile strength whereas in case of polymer matrix laminated composite it is 60-80% of its tensile strength.

(iii) **Damping characteristics:** The natural frequency of vibration not only depends on the shape of component but also depends upon square root of its specific modulus. Due to low weight, composite materials have high natural frequency and the resonance not occur easily.

(iv) **Corrosion Resistance:** Polymer matrix is not only a non-corrosive material but also save fibres from exposure to environmental conditions at normal temperature.

(v) **Material utilization factor:** Material utilization factor is the ratio of raw material weight to final part weight. Material utilization factor for metals varies from 15 to 20 whereas in case of composite it is varies from 1.2 to 1.3.

The main disadvantage of polymer matrix composite material is the temperature constraint. Polymer materials starts to defuse at higher temperature which reduces its application part. Hygrothermal aging of the polymer material when it is subjected to the water or to the thermal exposure is a critical issue, which reduces the durability of the material.

1.3 Applications

Since the development of fibrous, a composite material not only became an important engineering material for aerospace industry but was also important for civilian instruments. Light weight of composite material is the primary reason to use it for aircraft applications, which can not only reduce the cost of manufacturing but also improve the performance of

aircrafts. Equipment's like oil tanks, pipes to mass transfer or pumps are being manufactured by the anticorrosive materials, glass fibre reinforced plastic is an important anticorrosive material and used highly for these type of applications. There are also other several applications of composite materials due to its advantages over the traditional materials.

In real life applications, different components of the machines need to be joined together to perform the desired function and due to manufacturing and transportation limitations, there is requirement of efficient joining methods to join two or more different parts.

1.4 Types of Laminate Joints

There are three basic joining methods for the fiber reinforced composite materials *i.e.*, adhesive bonding, mechanical joint and hybrid joint (adhesive + mechanical). Out of three major joining methods, mechanical fastening is the most preferable joining method as it is simplest, less costly and facilitates disassembly to repair without destroying the basic components of the joint.

1.4.1 Adhesive joint

In adhesive joints, two substrates called as adherents are joined by means of adhesive materials. The advantage of adhesive joint is its strength, which depends on the properties of adhesive and adherents material. Cohesion of adhesive film and the adhesion of film to adherents play the major role to define the strength of the adhesive joint. The advantages of adhesive bonding technique are its ability to join dissimilar materials, cheapest to use and its sealing properties. But the disadvantages associated with this technique are the surface preparation of adherents before to apply adhesive film, disassembly of joint parts and the service temperature and environmental limitations, which narrows the application part of this technique.

1.4.2 Mechanical joint

Mechanical joint is used to connect two or more parts together temporarily or permanently but most of the time mechanical joint are required to disassemble for the repair or maintenance purpose. Single lap joint, double lap joint or butt joint are the some types of mechanical joints. Stress concentration, delamination during drilling of laminated composite and bolt-hole clearance are the factors that influence the failure of mechanical joints. Mechanical joints are insensitive to surface preparation, service temperature and humidity. Thus, the mechanical joint is still the dominant fastening technique used to join the composite structural laminates.

1.4.3 Bolted joint

It is a semi permeant mechanical joint in which nut, bolt and washers are used to assemble the basic components. Bolted joint is of two types, which can be classified on the basis of the

external force acting on the joint. If the line of action of external applied force is parallel to the bolt axes, the joint is called a tensile joint. If the line of action of external applied load is perpendicular to the bolt axes, the joint is called a shear joint. Shear joint has enormous applications in the assembly of different structural parts whereas in most of the cases tensile joint is used to clamp the two members together to prevent leakage.

The components of a shear bolted joint include the fastener and parts to be joined together. The preload exerted by the bolt is the primary feature of bolted joint. This initial clamping force ensures that the clamped parts remain in contact throughout the life of the joint and improve the performance of joint. Washers used in the joint also have a useful purposes. They minimize embedment of bolt head and nut into the clamped parts, aid in tightening and reduce stress concentration around the hole. The useful effect of washer is to distribute the initial axial preload over a large area of the clamped parts.

Design of bolted joint for polymer laminated composite materials is much more complicated than the design of joint for metals. Nature of composite material (in general orthotropic and brittle) results in complex fracture behaviour and number of failure modes. Therefore, it is important to study the different failure mode of composite joint for the optimal design of joint. Different types of failure modes are discussed below:

Bearing failure mode occurs when the bolt exerts the crushing force on laminate and laminate fails to resist it. The failure load can be calculated using equations (1.1) and (1.2).

$$A_r = d \times t \tag{1.1}$$

$$F = d \times t \times \sigma_b \tag{1.2}$$

Net-tension failure mode occurs along an axis perpendicular to the longitudinal axis. Width of specimen is responsible for the net tension mode of failure of laminate joint. The failure load can be calculated using equations (1.3) and (1.4).

$$A_r = (w - d) \times t \tag{1.3}$$

$$F = (w - d) \times t \times \sigma_t \tag{1.4}$$

Shear-out failure mode occurs along an axis parallel to the longitudinal axis. This type of failure occurs at low edge distance. The failure load can be calculated using equations (1.5) and (1.6).

$$A_r = 2 \times e \times t \tag{1.5}$$

$$F = 2 \times e \times t \times \tau_s \tag{1.6}$$

Where, A_r is the resisting area, F is the failure load, σ_b is the bearing strength, σ_t is the tensile strength, τ_s is the shearing strength, d is the diameter of hole, t is the thickness of plate, w is the width of plate, e is the distance from side edge to centre of the hole.

Fig. 1.1 shows the laminate failure mode in a single bolt joint *i.e.*, Net-tension, Shear-out and Bearing mode. Bearing failure mode is a desirable failure mode since it is less catastrophic one whereas net-tension and shear-out modes are catastrophic in nature which occurs without any warning and are to be avoided for safe designing.

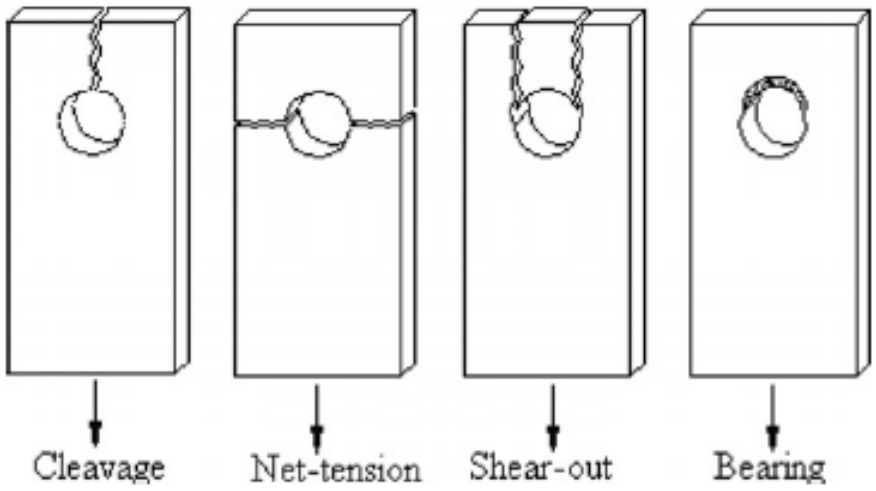

Fig. 1.1 Failure modes [2]

1.5 Mechanical behaviour of composite material and its joint

In comparison to conventional engineering materials, composite materials have different mechanical behaviour characteristics. Most commonly used engineering materials are homogeneous and isotropic, however this is not true in case of composite material. Generally composite materials are heterogeneous *i.e.*, properties are directional dependent and non-isotropic but in some cases it can be orthotropic or anisotropic. The ability of tailoring a composite material as per requirement makes it advantageous over a traditional material. By definition, isotropic materials have equal strength and stiffness in all directions but contrary to this composite material can be manufactured to have a more stiffness and strength in any particular direction as per requirement. This anisotropic nature (in general orthotropic) of composite material leads to different mechanical behaviour than that of isotropic materials. Testing criteria of composite material is also different than that of isotropic material, different ASTM standards are available to find out the orthotropic properties of composite materials.

But due to the stress concentration around the hole in mechanical joint, joint becomes the weakest member of the structure. In case of composite material stress concentration is not only the factor but the nature of material also becomes the dominant factor, which make it difficult to join. In case of bolt joint of composite materials research, the attention is given to determine

the effect of different parameters on the bearing strength of the joint [3]. Fig. 1.2 defines the different parameters which effect the bearing strength of composite bolted joint.

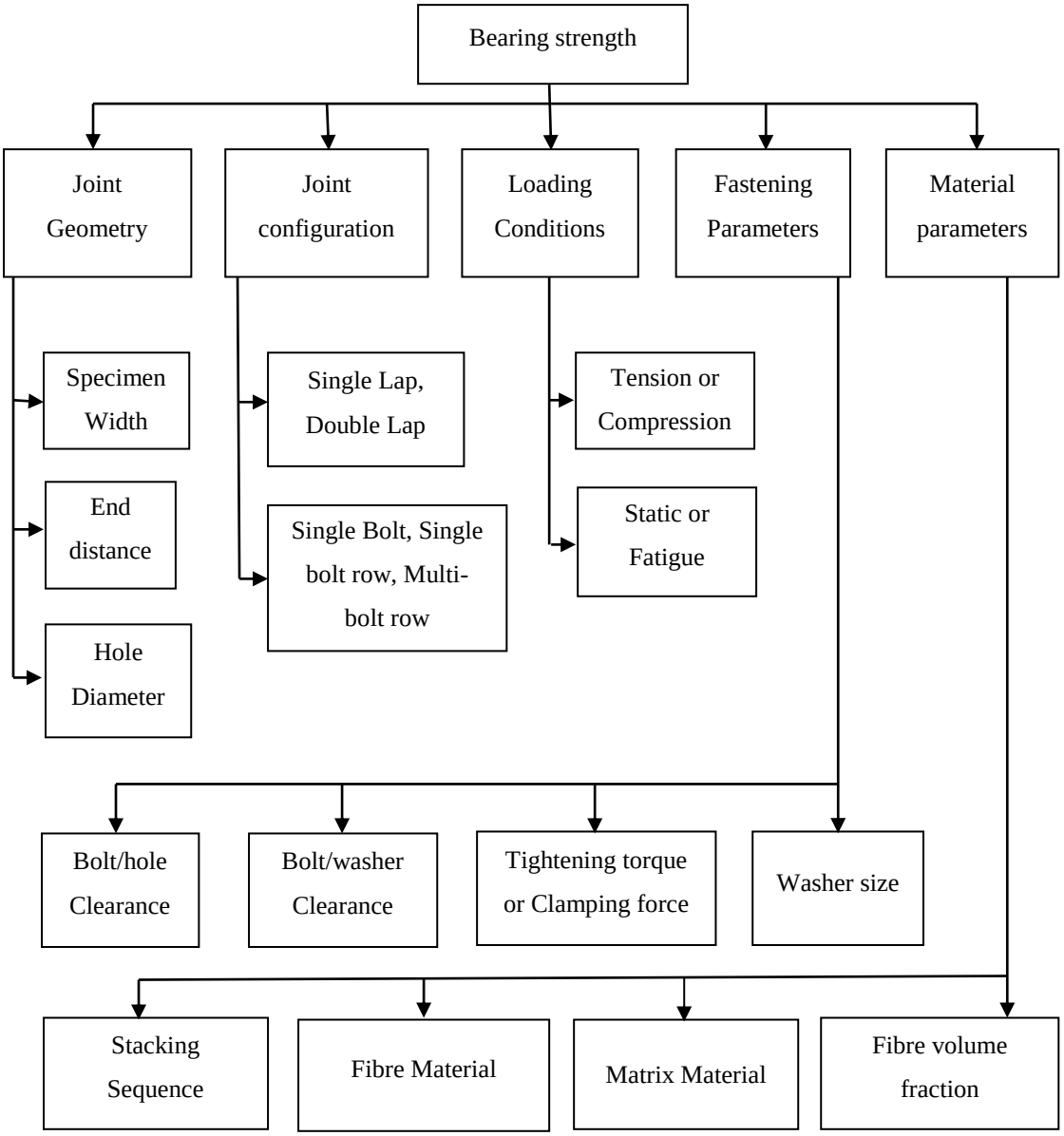

Fig. 1.2 Different strength parameters

CHAPTER 2

LITERATURE REVIEW

Mechanical joint is the weakest part of the structure due to stress concentration around the hole. Mechanical joints prepared from polymer composites has the lowest mechanical efficiency as compared to that of metal. So a lot of research is focused on this area to increase the strength of composite bolted joint and study the failure mechanism of joints. The following section gives a brief review of work done by different researchers on the analysis of bolted joints prepared from polymer composite laminates.

2.1 Literature review

Mechanical joints in laminated polymer composite material are discussed with the special attention on the study of bolted joints and its numerical simulation. There are number of parameters which effect the bearing strength of composite joint. The present section deal with the literature published by the different researchers to study these parameters of mechanical joint prepared from composite material.

Sen *et al.* [2] performed experimental study to determine failure mode and bearing strength of bolted joint under preload. Two different geometrical parameters, edge to hole diameter ratio (e/d) from 1 to 5 and width to diameter ratio (w/d) from 2 to 5 were chosen for this study. In order to calculate effect of material parameter on failure mode and bearing strength, three different stacking sequence groups $[0^\circ/0^\circ/45^\circ/-45^\circ]_s$, $[0^\circ/0^\circ/45^\circ/45^\circ]_s$ and $[0^\circ/0^\circ/30^\circ/30^\circ]_s$ were studied. Experimental result showed that the failure mode were changed as the preload increased from 0 to 3 Nm and 3 to 6 Nm. It was concluded that preload affects the bearing strength of joint significantly and the bearing strength with stacking sequence of group 2 was higher in comparison to other groups for the identical parameters.

Khashaba *et al.* [3] investigated the effect of tightening torque and washer outer diameter on the strength of glass fibre reinforced epoxy composites with the stacking sequence of $[0^\circ/\pm 45^\circ/90^\circ]_s$. Torque and washer outer diameter were chosen as 0, 5, 10, 15 Nm and 14, 18, 22, 27 mm respectively. Specimen with outer diameter 18 mm and 15 Nm torque gave the maximum bearing strength as compared to other combinations. Due to different strain in different layers of laminate, initially delamination was observed, followed by the net tension failure and shear out failure of laminas at 90° and 0° respectively.

McCarthy *et al.* [4] investigated the effect of bolt hole clearance on stiffness and strength of single bolt, single lap bolted joint numerically and experimentally. ASTM standard D5961

was used for the manufacturing of specimens in order to obtain the bearing mode of failure. Two torque levels were chosen for the analysis of protruding and countersunk bolted joint. Experimental results showed that the joint efficiency decreases as the bolt hole clearance increases. But in case of countersunk and fully torqued joint, strength of joint was found to be insensitive to clearance. Fig 2.1 shows the boundary conditions and the mesh used to evaluate the results numerically.

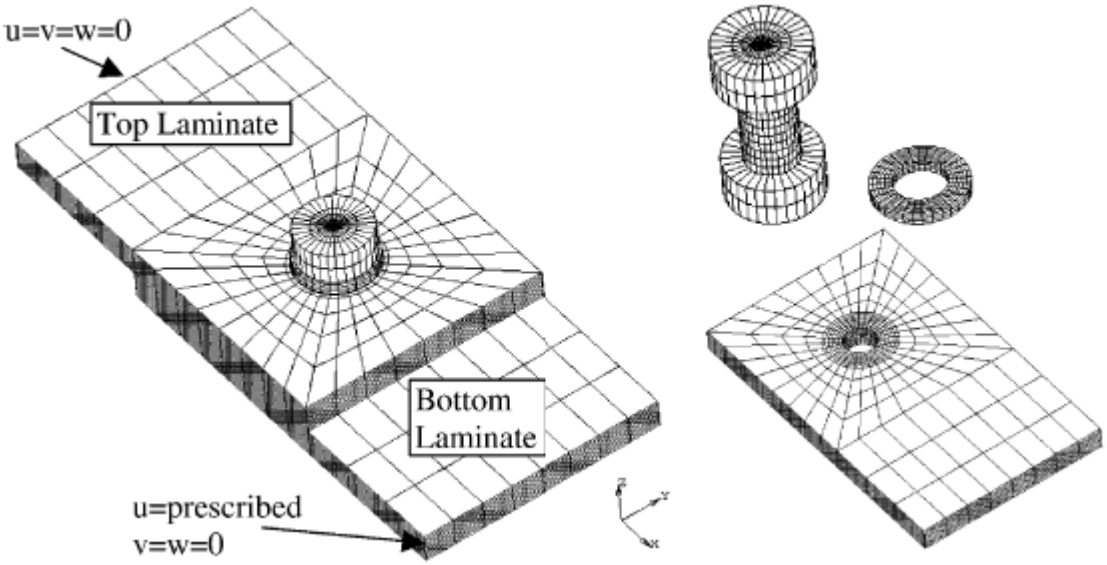

Fig. 2.1 FEM with boundary conditions [4]

Kweon *et al.* [5] presented a numerical method to determine characteristic lengths for the prediction of failure modes on characteristic curve around the hole of composite joint without any experimentation. Fig. 2.2 shows the characteristic curve around the hole.

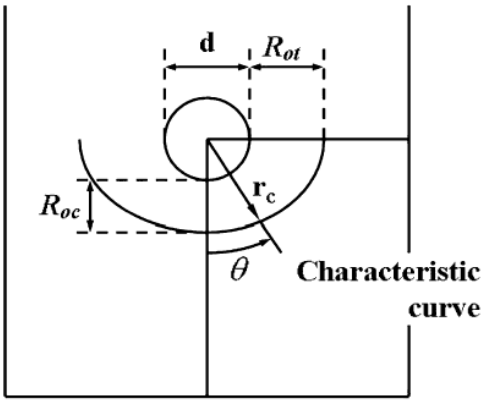

Fig. 2.2 Schematic diagram of characteristic curve [5]

In the study compressive characteristic length (R_{oc}) and tensile characteristic length (R_{ot}) was calculated numerically instead of experimentally. It was remarked that characteristic lengths were not changed until unless geometry or material of specimen is changed. When the tensile and bearing load is changed, the magnitude of stresses changed but stress distribution remains same, so the curve lengths were insensitive to applied load mentioned in the work. Failure analysis was done on the characteristic curve rather than on the bolt hole. This numerical study was validated by the 52 experimental test results and the good agreement between the experimental and numerical results was found to form a characteristic curve.

Xiao and Ishikawa [6] measured the bearing damage behaviour of composite bolted joints using acoustic emission technique. Non-contact electro-optical extensometer was used to measure the hole elongation. Two different matrix material *i.e.*, Polyamide and Epoxy, were selected to compare bearing strength and damage behaviour in carbon fibre reinforced composite. The load-displacement curve was examined with respect to acoustic emission characteristic and failure mechanism. It was concluded that the toughness of composite material had significant effect on its damage behaviour. Epoxy based matrix exhibited higher matrix cracks and delamination than polyamide matrix based laminates. But at the same time as compared to polyamide matrix based composite, epoxy matrix based composite pin joint showed higher failure strength due to the effect of different resin properties and interface bond strength.

Xiao and Ishikawa [7] developed the analytical model for simulating the bearing strength and failure behaviour of laminated composite bolted joint. Abaqus finite element code was used to implement the model. Progressive damage and nonlinear material behaviour were taken into account. Hashin and Yamada-Sun's hybrid failure criteria along with degradation model were used to analyse the stress distribution. Numerical simulation results agreed well with the experimental results.

Kelly [8] investigated the strength and fatigue life of hybrid (bolted/bonded) carbon fibre reinforced composite single lap joint. Stiffness, strength and fatigue life of hybrid joint were improved as compared to adhesive bonded joint. In the study of hybrid joint two different types of adhesives with low elastic modulus and high elastic modulus were used. Load sharing between bolt and adhesive was only observed in the hybrid joint with low modulus adhesive. This load sharing mechanism also changed the behaviour of hybrid joint to non-catastrophic failure. Fatigue life of hybrid joints with high modulus adhesive was increased whereas static strength of joint remained unchanged.

Liu *et al.* [9] calculated the effect of cure cycle on the properties of carbon fibre reinforced epoxy laminates. Unidirectional fibrous laminates were manufactured with stacking sequence$[0^{\circ}/90^{\circ}]_{3s}$. The series of experiments of short beam shear, three point flexural and tensile test were performed as per ASTM D2344, ASTM D790 and ASTM D3039 respectively. Results showed that the pressure should be applied when the viscosity of resin is minimum. In this cost effective cure cycle, exponentially decreasing relationship between void content and applied pressure were obtained. The results suggested that interlaminar flexural modulus is more sensitive to void than the tensile strength, whereas tensile modulus is not sensitive to void content.

Nassar *et al.* [10] investigated the behaviour of single lap double bolt in serial composite joint experimentally. Two bolt in series were considered in composite to composite and composite to aluminium joint configurations. For the experimentation woven glass/epoxy laminates were prepared as per the geometric configuration of ASTM D5961. To study the bolt-tightness, four tightening configurations as lower bolt tight-top loose, lower loose-top tight, both top and lower loose and both top and lower tight were used. Experimental result concluded that the failure load increased when torque on at least one bolt increased. Whereas the joint stiffness increased when both top and lower bolt were fully tightened.

Asi *et al.* [11] determined the effect of linear density of woven glass fibre on the bearing strength of glass fibre reinforced epoxy laminated composite mechanical joint. Reinforcement of woven glass fibre into epoxy resin matrix with three different linear densities *i.e.*, 200, 270 and 300 g/m^2 were used. Void content in laminate was calculated as per ASTM D2734-94. Tensile and compression tests were conducted according to ASTM D3039-76 and ASTM D3410-87 respectively. It was observed that void content has the adverse effect on the mechanical properties of composite. Fibre volume fraction and void content of laminate increased with increase in linear density of woven fibre. Bearing strength of composite pin joint first increased with increase in linear density and then decreased due to higher value of void content.

Irisarri *et al.* [12] developed the refined finite element model to predict the bearing strength of single fastener joint in carbon fibre reinforced plastic composites. In this model effect of delamination on bearing strength of mechanical joint were taken into account by means of cohesive elements. Progressive damage and viscoelastic models were combined to analyse the ply behaviour. Non-linear behaviour of matrix, matrix failure, delamination and fibre failure were considered to develop the progressive damage model. Experimental result validated the

proposed model as it was capable to predict the joint behaviour and strength with respect to stacking sequence.

Egan *et al.* [13] used nonlinear elements in abaqus code to model single lap, single bolt countersunk composite joint. Quasi-isotropic carbon/epoxy laminate with stacking sequence $[45^{\circ}/0^{\circ}/-45^{\circ}/90^{\circ}]_{5s}$ were used. The geometric parameters of model were chosen as w/d = 6, e/d = 3 and t/d = 1.3 as given in ASTM D5961 standard. Effect of clearance on properties of joint was studied in this model. Loss in joint stiffness was reported as the bolt-hole clearance increased. The finger-tight bolt pretension induced through thickness stresses in the shank of the fastener, while compressive stresses were observed in the laminate under the head of bolt and washer.

Qin *et al.* [14] studied the effect of protruding head and countersunk fastener on the mechanical behaviour of double lap composite bolted joint. Christensen's equation was used to calculate transversely isotropic material properties. Experiments were carried out to find out strength and stiffness of double lap joint under the effect of different fasteners. Initially stiffness, before the damage onset was same for both type of fastener configurations, but as the joint nonlinearity occurred, joint stiffness of countersunk joint was recorded more than that of protruding head joint.

Gray *et al.* [15] performed experiment on single lap, multi-bolt countersunk composite mechanical joint to estimate the stiffness and strength of the joint with respect to laminate thickness and tapering of laminates. It was observed that laminate thickness has significant effect on strength and stiffness of joint, as the thickness increases both strength and stiffness increases. To reduce the weight of structure, thickness of laminate outside the overlap region was reduced which did not affect the ultimate load carrying capacity of the joint. Effect of missing fastener was also calculated in this study and result showed the significant reduction in load carrying capacity of joint with respect to reference joint design.

Zhai *et al.* [16] investigated the bearing strength and joint efficiency of single lap, single bolt countersunk laminate composite joint. Specimens were manufactured as per standard ASTM D5961 by using carbon fibre reinforced epoxy composites with quasi isotropic lay-ups. Digital image correlation (DIC) system was used to calculate bearing strength under the effect of bolt torque and bolt-hole clearance. In experiments it was observed that bolt torque delays joint stiffness loss whereas bolt-hole clearance leads to an earlier joint stiffness loss. Increasing the bolt-hole clearance reduced contact area between bolt and hole which lead to reduction in joint stiffness.

Sekhon *et al.* [17] compared the strength of glass fibre laminated composite pin joint made with two different nanoparticles *i.e.*, nano TiO_2 and nanoclay. The influence of geometrical parameters edge-to-hole distance (e/d) and width-to-hole distance (w/d) were evaluated experimentally and numerically. It was concluded that the maximum joint strength was obtained at 3wt.% of clay and 2wt.% of nano TiO_2. Desirable progressive bearing mode of failure was observed at $w/d \geq 4$ and $e/d \geq 4$ for specimens of nanoclay whereas in case of TiO_2 specimens, it was observed at $w/d \geq 4$ and $e/d \geq 5$.

Mara *et al.* [18] studied the effect of metallic insert in drilled hole, on the stiffness and bearing behaviour of joints. E-glass roving with stacking sequence $[0/90, \pm 45, 0/90, \pm 45, 0/90]_s$ was used as the reinforcement in polyster matrix. Fig 2.3 shows the mechanism of pre-tension load transfer with or without insert in hole.

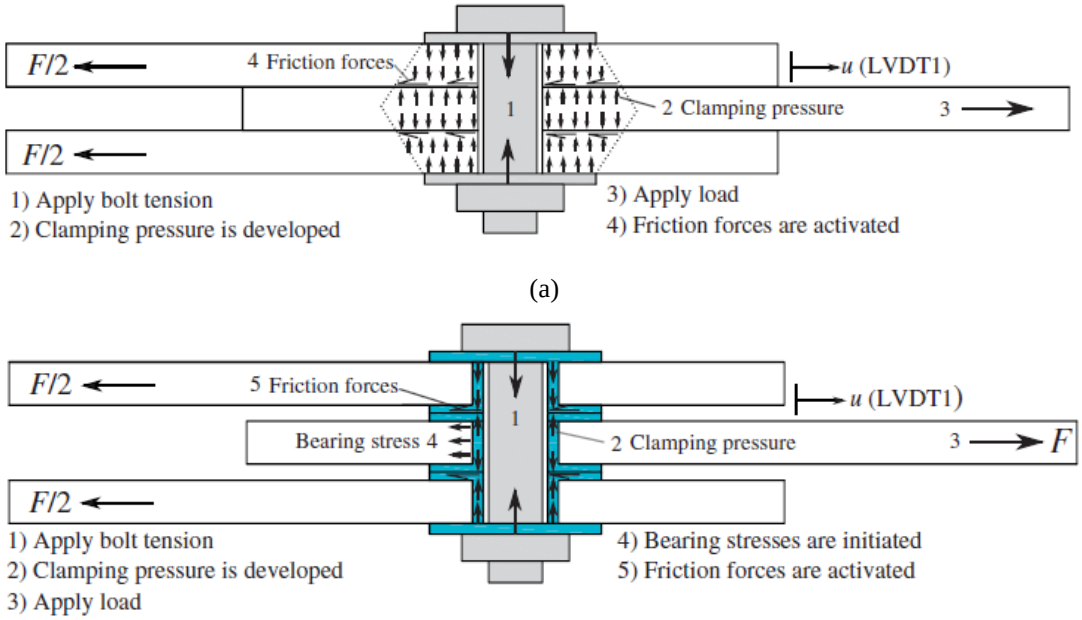

Fig. 2.3 Load transfer mechanism (a) Bolted joint with pretension bolt (b) Bolted joint with insert and pretension bolt [18]

It was demonstrated that in the form of stiffness and strength, joint efficiency of double lap joint increase with the use of metallic insert. It was observed that increasing the bolt pretension, increased the strength and stiffness of joint. Although used fibre reinforced composite material was viscoelastic which result in bolt pretension relaxation but the use of insert reduced the pretension loss with respect to time and loading.

Singh *et al.* [19] investigated the effect of nanoclay on failure mode and strength on unidirectional glass fibre reinforced epoxy composite pin joint. Significant effect of wt.% of

nanoclay and geometric parameters on bearing strength and failure mode were observed numerically and experimentally. Characteristic curve method was used to predict the failure mode. Tsai-Wu failure criteria along with progressive damage analysis showed agreement between experimental and numerical results.

Yao *et al.* [20] studied basalt FRP/steel single lap adhesive joint under the effect of different loading rates and temperature. For the experimentation loading speeds were selected as 0.625, 1.25, 2.5 and 5 m/s and temperature range was selected as -25˚, 0˚, 25˚, 50˚ and 100˚C. The effect of loading rate and temperature on the bond strength was estimated. Experimental result showed that the bond strength increased by increasing the loading rate and temperature from -25 to 50˚C but decreased as the temperature increased further from 50 to 100˚C.

Aldajah *et al*. [21] studied the effect of sea and tap water exposure on the mechanical properties of symmetric and anti-symmetric glass fibre reinforced polymer (GFRP) composite laminates. Three point bending test as per ASTM D790 is used to test the specimens before after the aging. It was concluded that total 60% loss of flexural stiffness in symmetric laminate and 28% loss of flexural stiffness occurs in anti-symmetric laminate when both were subject to sea water for 2000 hours. Under the identical conditions when the specimen were tested after the aging in tap water, flexural stiffness was reduced by 55% and 29.4% in symmetric and anti-symmetric laminates respectively. It was also observed that the maximum loss of flexural stiffness occurs within the first 500 hours.

Alawsi *et al.* [22] studied the effect of environmental conditions on the mechanical properties of symmetric and anti-symmetric glass fibre reinforced composite laminates. In order to measure the effect of humidity on the flexural stiffness and strength, samples were put into the highly humidity conditions for 2000 hours and then aged samples were tested using three point bending test as per ASTM D790-02. It was concluded that humidity exposure to GFRP had adverse effect on its mechanical properties. After the exposure of 2000 hours to humidity, flexural stiffness of symmetric GFRP composite was reduced by 54% whereas for anti-symmetric it was reduced by 27%. Same trend was also noticed in case of flexural strength of GFRP, which were reduced by 19% of symmetric and 7% of anti-symmetric laminates.

Mourad *et al.* [23] calculated the effect of seawater on the physical bonds at interface, failure mechanism and on the mechanical properties of glass reinforced epoxy and glass reinforced polyurethane composites. The effect were studied with respect to time period of three months, six months and one year, at the room temperature and at the 65˚C temperature. It was observed that the immersion of seawater was increased as the time of immersion and temperature

increases. It was cleared from SEM images that matrix protect the fibres from corrosive elements in seawater but moisture breakdown the chemical bonds at the interface of fibre and matrix, which reduces the tensile strength by 19% at room temperature and 31% at temperature of 65˚C after one year. Ductile failure of matrix took place due the moisture absorption of matrix material.

Soykok *et al.* [24] investigated the effect of hot water aging on the behaviour of composite joint. Specimens were prepared as per ASTM D5961-01 with stacking sequence of $[0^{\circ}/90^{\circ}/45^{\circ}/-45^{\circ}]_s$ and glass fibre reinforced epoxy composite material. Effect of water temperature and time on bearing strength of joint was studied. 50˚, 70˚ and 90˚C temperature for 1 and 2 week time period were selected for aging parameters. Experimental results showed that the aging time and temperature have a significant effect on mechanical properties of composite material. But strength reduction at a temperature of 90˚C is more than that of at 70˚C. Preloading of joint exhibited the same positive trend toward strength as it showed without aging.

Soykok *et al.* [25] determined the effect of thermal conditions and preload on failure behaviour of single lap glass fibre reinforced epoxy composite mechanical joint. Load carrying capacity of mechanical joint at 40˚, 50˚, 60˚, 70˚ and 80˚C temperature was studied. Due to increase in temperature, internal energy of composite material increases and molecular movement of material becomes easier which degrade the material. As compared to strength at room temperature maximum decrease in failure load was observed to be 55% and 70% at the temperature of 70˚C and 80˚C respectively. Experimental result showed that the temperature had adverse effect on load carrying capacity of joint but it does not alter the failure mode, which is highly affected by material and geometrical parameters.

Larbi *et al.* [26] studied the effect of hygrothermal aging on mechanical properties of carbon fibre reinforced epoxy and E-glass fibre reinforced vinylester composite materials. Both materials were tested after the exposure of two different environments, the sea water and the distilled water at a temperature of 40°C. It was noted that due to high value of pH of seawater, absorption in seawater is more than that in distilled water which degrade the matrix material continuously. Three point bending test was performed to calculate flexural modulus of specimen before and after aging. The loss of tensile strength and flexural modulus was recorded after the hygrothermal aging of specimen.

2.2 Conclusion of literature review

It was observed from literature review that there are number of parameters such as joint geometry, materials used to prepare laminate, its volume fraction, stacking sequence, joint configuration, fastening parameters, hygothermal aging and the type of loading which affects the ultimate failure load and failure mode of the composite laminate joints. Fastening parameters such as bolt pretension and washer size can be very effective on the joint efficiency and failure mechanism. Hygrothermal aging decrease the durability, modulus and strength of the polymer composite material as well as its joint. Hence, the present work deals with the numerical analysis of bolt joint and its experimental validation.

The objectives of the present work are:

(i) To fabricate glass fibre reinforced composite laminates and its characterization using SEM and UTM.

(ii) To fabricate single bolt, single lap joint from the prepared composite laminate and investigate the effect of bolt pretension and washer on joint performance.

(iii) Numerical analysis of the joint and validation with experimental results.

CHAPTER 3

EXPERIMENTATION

In case of bolted joint, geometric parameters such as width-to- hole ratio, edge distance-to-hole ratio and fastening parameters such as torque and washer size are effective to joint failure load, its efficiency and failure mechanism. To evaluate the effect of these parameters the performance of joint, single lap joints have been prepared using woven glass epoxy composite laminates. This chapter deals with the preparation of laminated polymer composite material and performance analysis of bolt joint.

3.1 Materials

Materials such as Fibre, Resin, Hardener, Accelerator and Acetone are used to prepare the composite laminates. The properties and composition of these materials are explained below in detail.

3.1.1 Glass fibre

Two dimensional woven glass "Advantex" fibre with 360 gsm was supplied by Owens Corning India Pvt. Ltd., Mumbai. Table 3.1 shows different properties of woven glass fibre used.

Table 3.1 Properties of the woven glass fiber

Description	**Fibre type**	**Density (g/cm^3)**	**Area density (g/m^2)**	**Tensile strength (g/mm^2)**	**Tensile modulus in tension (GPa)**	**Elongation at breaking load (%)**
Woven Glass fibre	Advantex E-glass	2.62	360	3100-3800	80-81	4.6

3.1.2 Resin

Matrix is adhesive bonding material which is used to prepare the laminated composite material. Resin is a highly viscous substance which is typically convertible into polymers. Resin are the mixtures of organic compounds. Epoxy resin, hardener and accelerator altogether have been used to prepare the matrix and are supplied by Atul Ltd., Gujarat, India. The mechanical and physical properties of matrix are given in Table 3.2 and 3.3 respectively. Table 3.2 shows the mechanical properties of resin when epoxy (L-12) and hardener (K-12) are mixed in the ratio of 1:1.

Table 3.2 Mechanical Properties of epoxy based resin

Description	Specific Gravity	Elastic Modulus in Tension (N/mm^2)	Tensile Strength (N/mm^2)	Flexural Strength (N/mm^2)	Compressive Strength (N/mm^2)
L-12(100)+k-12(100)+k-13	1.80-1.85	15000-16000	70-90	100-120	190-210

Table 3.3 Physical Properties of epoxy based resin

Description	Density (g/cm^3)	Viscosity (mPa-s)
Resin (L-12)	1.1-1.2	9000-12000
Hardener (K-12)	1.15-1.25	150-230
Accelerator (K-13)	0.88-0.92	<10

3.1.3 Acetone

Acetone is a solvent with molecular formula $(C_3H)_2CO$ and is used as supporting material to clean the equipment's *i.e.,* beakers and the Teflon sheets.

3.2 Composite Preparation

Laminated composite is an assembly of laminas which are assembled to provide the required properties such as strength and stiffness. These properties of laminate composite not only depends on material of which it is made but also depends upon its geometrical parameters [27]. Specimens were manufactured under the guidelines of ASTM D3039. In the pilot study it was determined that 9 laminas gave the thickness of 2.5 mm as required for ASTM D3039. The detailed procedure of manufacturing of composite laminate is discussed below:

3.2.1 Cutting of glass fibre

Cutting of glass fibre is as simple as the cutting of other familiar materials. But the little preparation and appropriate tools are required. Glass fibre is cut from the roll to the adequate

size which can fit into compression moulding machine. Fig. 3.1 details the marking and cutting of the lamina with the size of 180×180 mm.

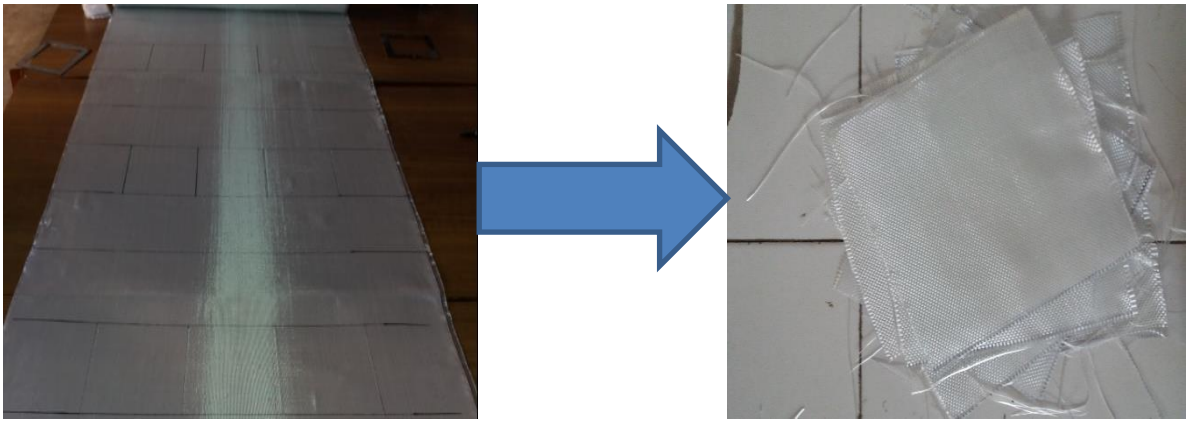

Fig. 3.1 Cutting of glass fibres

3.2.2 Preparation of Resin

Epoxy resins can be cross-linked by themselves through catalytic polymerisation or the co-reactant's hardener used to complete the reaction of cross-linking which is called as curing. This reaction of epoxy resin with hardener form the thermosetting polymers which have very good thermal and mechanical properties. In order to obtain a 60:40 volume fraction ratio of fibre to matrix; 126 gm weight of fibres (in the laminas) requires 84 gm weight of resin. So, the 40 gm of resin was mixed with 40 gm of hardener in the ratio of 1:1. 2% accelerator was used to increase the curing rate of resin.

3.2.3 Hand Lay Up Technique

Hand layup technique is the simplest and inexpensive technique. Simple processes of hand layup technique requires least amount of equipment. Fig. 3.2 shows the hand layup technique, in which prepared resin is applied on the Teflon sheet by using the brush and the fibre lamina is placed on it. Pressure roller is used to flatten the lamina and to remove the entrapped air so that void or porosity can be removed. The resin is again applied by using brush and another lamina is placed on it. This procedure is repeated several times to get the final thickness of laminate to 2.5 mm with 9 layers of woven fibre. After lay-up, laminates are cured at room temperture for 36-48 hours depending upon the enviourement conditions.

Fig. 3.2 Hand layup technique

3.2.4 Compression moulding

Compression moulding is the most common technique which can produce a wide variety of composites from small to large. It is simplest method of composite moulding in which after curing at room temperature, the laminates are placed between two hot plates of compression moulding machine and pressed at a particular temperature. Pressure is applied to consolidate the laminate and to remove excess resin and voids [27]. Fig. 3.3 shows the compression moulding setup used in the present work. To mould the laminate, temperature of hot plates was increased to 150˚C and then 140 kN force was applied to remove the voids from the laminate. The laminate was kept at this temperature for 30 minutes and were cooled to the atmospheric temperature before removing from the machine.

Fig. 3.3 Compression moulding machine

3.3 Characterisation of material

Characterisation of material is a process in which the properties and structure of material is investigated. It is very difficult to estimate the material behaviour without characterising it. So the characterisation of material is important before it can be used. There are many techniques which are available to characterise the manufactured materials. Following is the characterisation of the manufactured woven glass fibre reinforced composite material by a microscopic technique and experimentation.

3.3.1 Scanning Electron Microscopy

SEM is the microscopic technique in which beam of electrons is focused on the surface of specimen to produce its image. The raster scan pattern is used to scan the surface of specimen by electron beam. The interaction of electrons with the atoms of specimen, produces the secondary electrons emitted by the atoms of specimen. These emitted secondary electrons can be detected by a special detector. On the basis of secondary electrons, detector produces an image which defines the topography of the specimen.

The woven glass fibre reinforced epoxy specimen were tested using the SEM technique. Fig. 3.4 shows the distribution of glass fibre in epoxy matrix and indicates the perfectness of the manufacturing process under which the specimens were prepared.

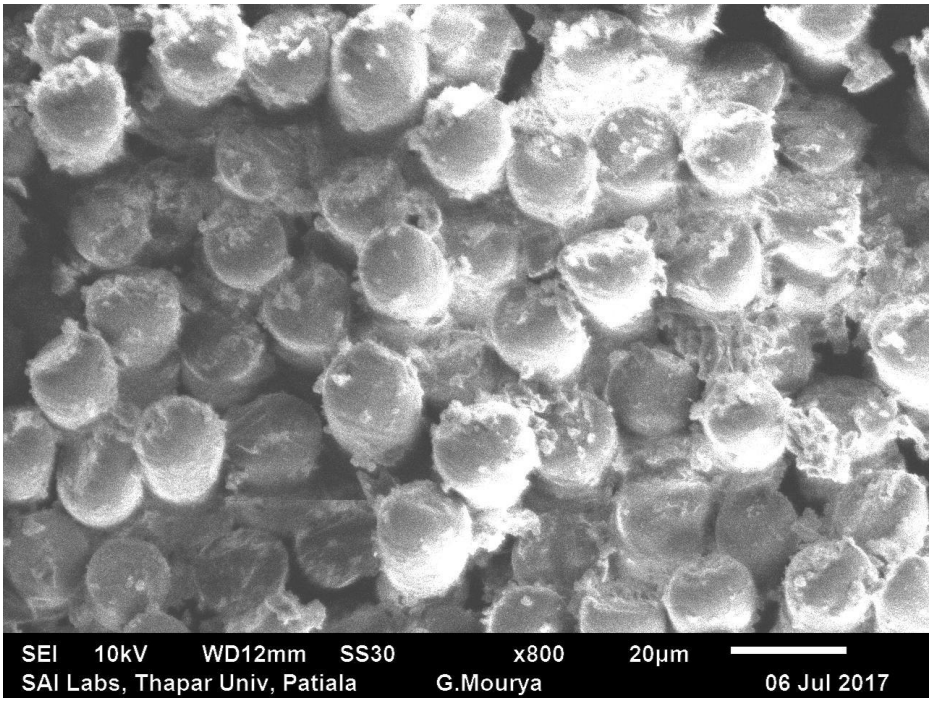

Fig. 3.4 SEM of fibre reinforced laminate

3.3.2 Calculation of volume fraction

The volume fraction of prepared composite laminate was calculated using ignition loss method as per ASTM D2584-11[28]. Fig. 3.5 shows the sample used for ignition loss method.

(a) (b)

Fig. 3.5 (a) Muffle furnace (b) Tested sample in desiccator

In this method, the weighted sample was placed in a muffle furnace at a temperature of 565˚C for 10 minutes. After the diffusion of matrix at a high temperature, only fibre remained in the crucible which was again weighted. Volume fraction was calculated using weight fraction as per equation (3.1). The weight fraction of matrix and fibre were found to be 0.28 and 0.72, respectively.

$$V_F = \frac{{W_F}/{\rho_F}}{{W_F}/{\rho_F} + {(1-W_F)}/{\rho_m}} \tag{3.1}$$

Where, V_F is volume fraction of fibre, W_F is weight fraction of fibre, ρ_F is density of fibre and ρ_m is density of matrix.

By using the equation (3.1) the volume fraction of fibre was calculated as 0.62 and the remaining was assumed the matrix content of composite material.

3.3.3 Mechanical properties of laminates

Mechanical properties *i.e.*, strength and modulus of laminate composite materials, were tested as per ASTM standards. Tensile strength and modulus were calculated as per ASTM D3039 [29]. Shear and compression properties were evaluated as per ASTM D732 and ASTM D695, respectively. ASTM D790 [30] was used to calculate the flexural properties of the prepared

laminates. Fig. 3.6 shows the Zwick-Roell Universal testing machine, Germany used for the mechanical characterisation of material.

Fig. 3.6 Universal testing machine setup

Table 3.4 shows the list of properties of prepared laminate. It was observed that due to woven configuration of fibre, longitudinal and transverse properties of the laminate are almost the same.

Table 3.4 Mechanical properties of laminate

Mechanical Property	Symbol	Magnitude
Longitudinal strength in tension	X_t	428 MPa
Transverse strength in tension	Y_t	428 MPa
Longitudinal strength in compression	X_c	270 MPa
Transverse strength in compression	Y_c	270 MPa
Shear strength	S_{12}	104 MPa
Flexural Strength	σ_f	671 MPa
Longitudinal modulus	E_{11}	21.68 GPa
Transverse modulus	E_{22}	21.68 GPa
Poisson ratio	ν_{12}	0.148

3.4 Preparation of Bolt Joints

The bolted joint consist of bolt and the parts to be jointed together. The use of bolted joint in the composite structural applications increases continuously. But composite bolted joints at its best reach a joint efficiency of 40-50% in terms of ultimate strength whereas in case of metal

alloys joint efficiency lies between 70-80%. Moreover weight efficiency of mechanical joint in laminated composite material show even lower performances as compare to it in metals [31]. As discussed earlier, there are some other geometric and fastening parameters which effect the performance of bolted joint. The present study deals with the effect of geometric parameters and fastening parameters on the joint efficiency and stiffness of single lap single bolt joint. A single lap bolt joint specimen geometry is shown in Fig. 3.7. In the figure, d is the diameter of hole, e is the hole to edge distance, w is the width, t is the thickness of the specimen and D is the outer diameter of washer.

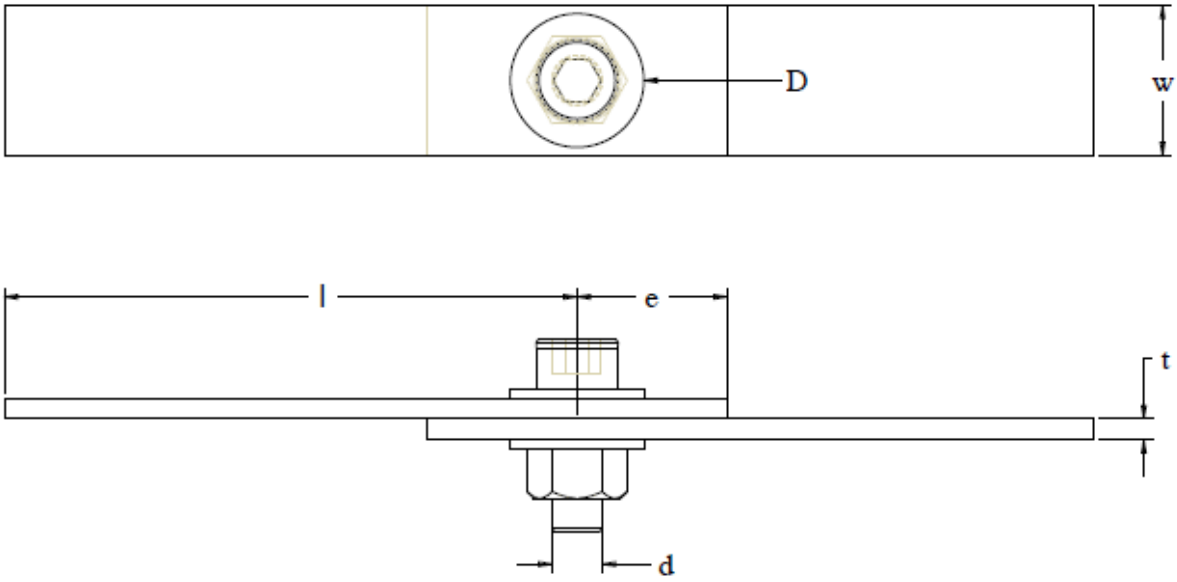

Fig. 3.7 Geometric parameters of single lap single bolt joint

The single lap single bolt joints were prepared using different geometrical and fastening parameters shown in Table 3.5. To estimate the effect of outer diameter washer on failure load, joint stiffness and joint efficiency, two levels of outer diameter *i.e.*, 12 mm and 16 mm have been studied. Bolt pre-tension is chosen to zero for studying the worst loading conditions and taken as 5 Nm to investigate fully clamped conditions. To estimate the effect of geometric parameters e/d and w/d ratio are varied from 3 to 4 and 3 to 5 respectively.

Bolted joint without washer and bolt pre-tension behave as a pin joint configuration to compare the joint efficiency with that of bolted joint configuration. Bolt with the shank diameter of 6 mm and inner diameter of washer as 6.02 mm were used in the present work.

Table 3.5 Different configurations of joint

Specimens	w/d ratio	e/d ratio	d (mm)	w (mm)	e (mm)	Torque (Nm)	Washer outer diameter (mm)
1	3	3	6	18	18	0	No
2	3	3	6	18	18	0	12
3	3	3	6	18	18	0	16
4	3	3	6	18	18	5	12
5	3	3	6	18	18	5	16
6	4	3	6	24	18	0	No
7	4	3	6	24	18	0	12
8	4	3	6	24	18	0	16
9	4	3	6	24	18	5	12
10	4	3	6	24	18	5	16
11	5	3	6	30	18	0	No
12	5	3	6	30	18	0	12
13	5	3	6	30	18	0	16
14	5	3	6	30	18	5	12
15	5	3	6	30	18	5	16
16	3	4	6	18	24	0	No
17	3	4	6	18	24	0	12
18	3	4	6	18	24	0	16
19	3	4	6	18	24	5	12
20	3	4	6	18	24	5	16
21	4	4	6	24	24	0	No
22	4	4	6	24	24	0	12
23	4	4	6	24	24	0	16
24	4	4	6	24	24	5	12
25	4	4	6	24	24	5	16
26	5	4	6	24	30	0	No
27	5	4	6	24	30	0	12
28	5	4	6	24	30	0	16
29	5	4	6	24	30	5	12
30	5	4	6	24	30	5	16

3.5 Results and Discussion

Fig. 3.8 shows the testing of the single lap bolted joint on the Zwick-Roell Universal Testing Machine, Germany. Tensile testing of single lap bolted joint at a temperature 25 ± 2°C as per the ASTM D3039[29] standard.

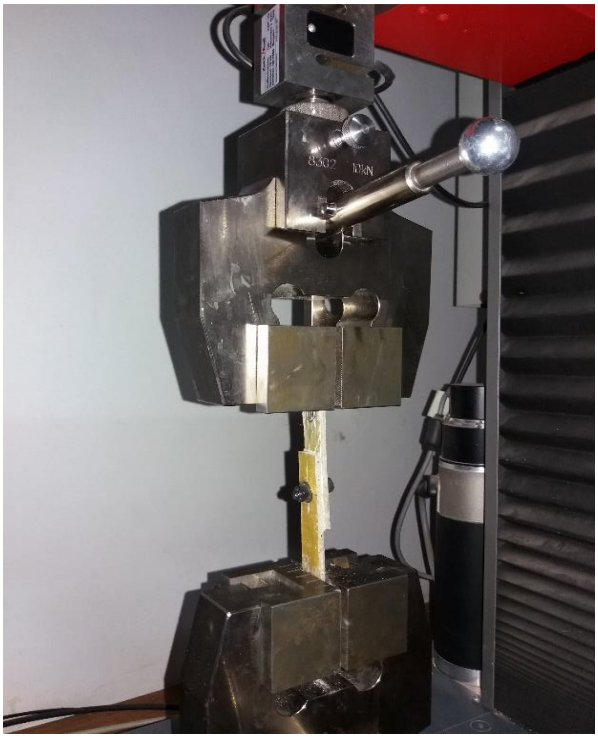

Fig. 3.8 Testing of specimen

The following are the load-displacement curves which are obtained during the testing of single lap, single bolt joint under different configurations.

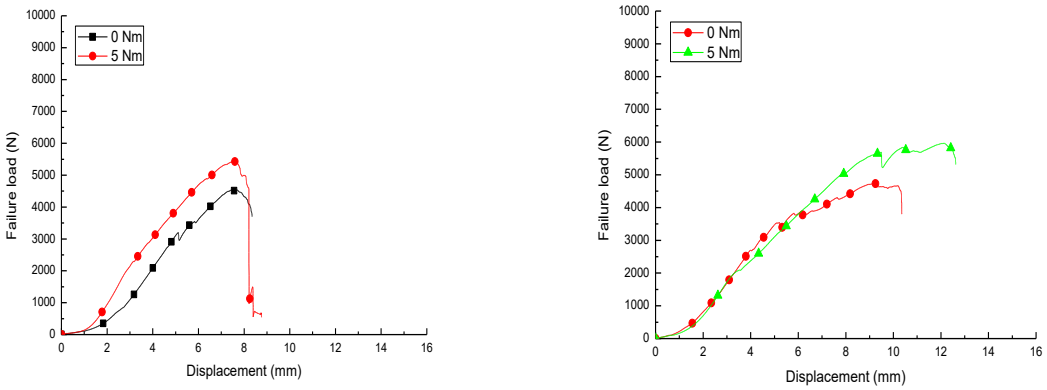

(a) (b)

Fig. 3.9 Load versus displacement curve for w/d = 3, e/d = 3 (a) Washer 12 mm (b) Washer 16 mm

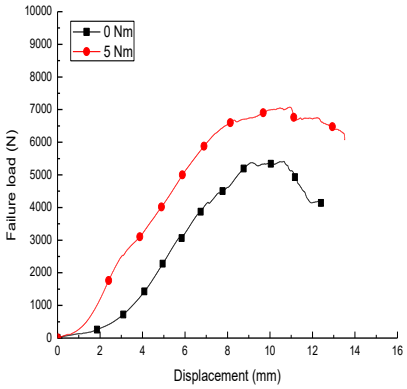

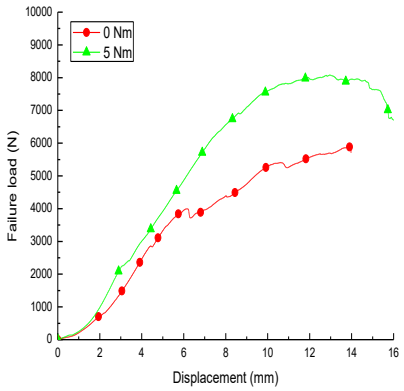

(a) (b)

Fig. 3.10 Load versus displacement curve for w/d = 4, e/d = 3

(a) Washer 12 mm (b) Washer 16 mm

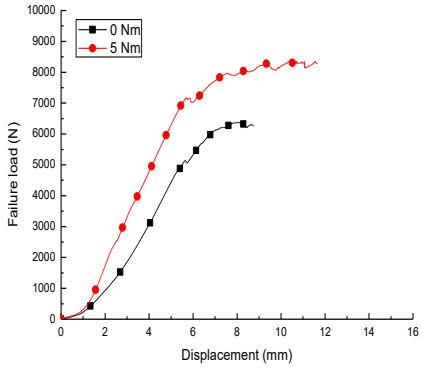

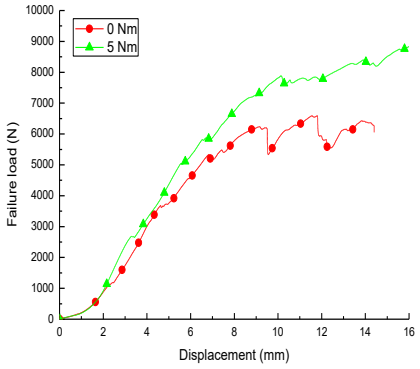

(a) (b)

Fig. 3.11 Load versus displacement curve for w/d = 5, e/d = 3 (a) Washer 12 mm

(b) Washer 16 mm

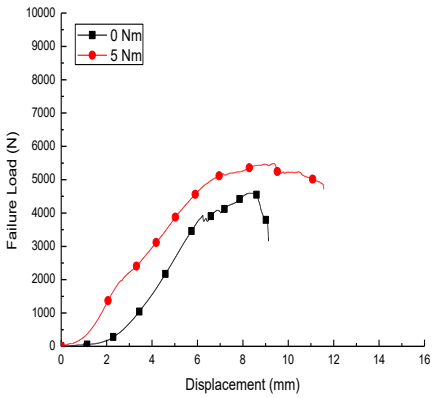

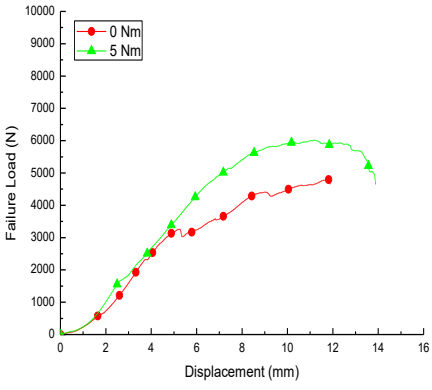

(a) (b)

Fig. 3.12 Load versus displacement curve for w/d = 3, e/d = 4 (a) Washer 12 mm

(b) Washer 16 mm

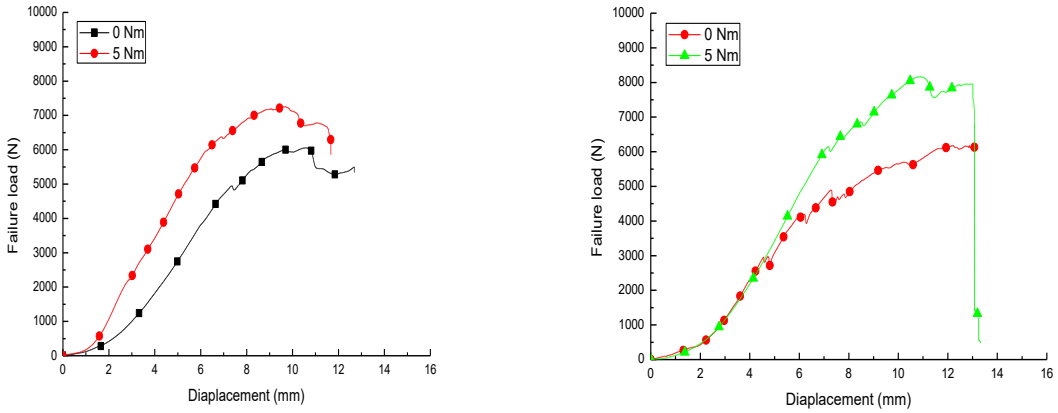

(a) (b)

Fig. 3.13 Load versus displacement curve for w/d = 4, e/d = 4 (a) Washer 12 mm (b) Washer 16 mm

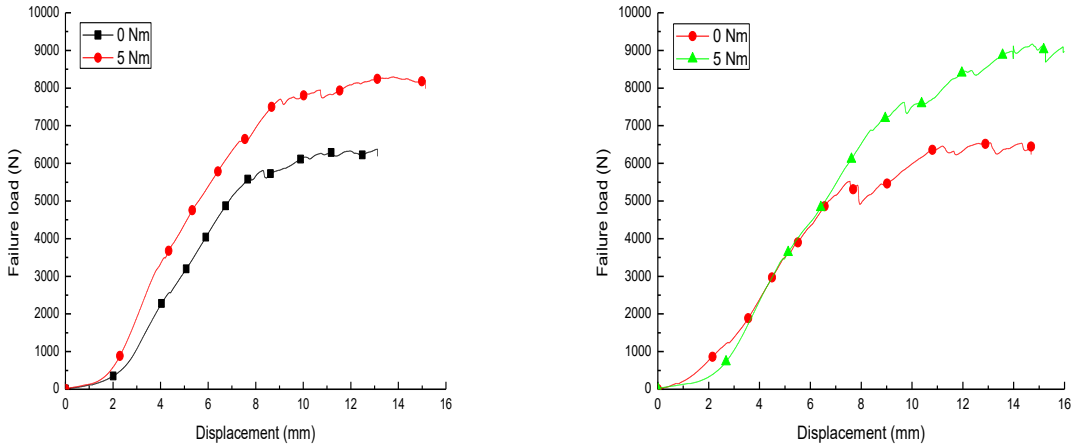

(a) (b)

Fig. 3.14 Load versus displacement curve for w/d = 5, e/d = 4 (a) Washer 12 mm (b) Washer 16 mm

It is clear from the fig. 3.9 to fig. 3.14 that the load-displacement curve were initially straight. But after initial failure, load-displacement curve depicts the non-linear behaviour *i.e.*, strain rate is more than the stress rate without predictable pattern. This non-linearity may also be associated to the change in contact area due to the secondary bending of laminates, caused by eccentric loading. For specimen with w/d = 3 along with e/d = 3 to 4, net-tension failure mode is observed for 0 Nm as well as 5 Nm. Similarly at w/d = 5 along with e/d = 3 to 4, bearing mode of failure is observed for 0 Nm as well as 5 Nm. But at a w/d = 4 along with e/d = 3 to 4, different failure mode was observed at both torque levels. For this configuration at a 0 Nm

torque level bearing mode of failure is observed whereas at torque 5 Nm net-tension mode of failure is observed. Comparing joint configurations with w/d = 3 and w/d = 4, it is observed that the maximum displacement before catastrophic failure for specimen with w/d = 4 is high, which is due to comparatively higher load bearing capacity and out of plane displacement of the specimen with w/d = 4. However, specimen with w/d = 3 failed more suddenly compared to specimen with w/d = 4. Failure mode of the specimen with w/d = 3 is pure net tension, whereas the specimen with w/d = 4 shows out of plane displacement before failing in net tension. Increasing e/d = 3 to e/d = 4 there is no significant difference in the maximum failure load of the joint. Initial failure load and the ultimate failure load both increase with increase in bolt pretension. But as the outer diameter of washer increases for the identical conditions, initial failure load decreases and failure of joint becomes more progressive than with the washer of outer diameter 12 mm. With the increase in outer diameter, confinement area of washer increases which results in wider damage area. It was observed that as w/d ratio increases, it delay the stiffness loss of single lap joint. Specimen with w/d = 3 fails in catastrophic manner. The specimen with washer at w/d = 4 and 5 at zero torque shows bearing failure, but the reduction in stiffness after the initial failure in the specimen of w/d = 5 is less than that of at w/d = 4. It is due to the reason that the large width offers more resistance to the secondary bending of joint due to eccentric loading.

3.5.1 Comparison of joint efficiency at different parameters

Efficiency (η) of bolted joint may be defined as the ratio of strength of bolted joint to the strength of solid plate [32].

$$\eta = \frac{R_P}{R_S} \tag{3.2}$$

Where, R_P is resistance of plate per pitch length and R_S is resistance offered by the solid plate. Equation (3.2) is used to evaluate the joint efficiency which is shown in the fig. 3.15 and fig. 3.16 corresponding to e/d = 3 and e/d = 4, respectively. The decrease in efficiency when the w/d ratio changes from 3 to 4, reveals that load carrying capacity of joint does not increase as much as the load carrying capacity of laminate solid plate increases. Maximum efficiency was recorded at w/d = 3 with 5 Nm bolt preload and washer outer diameter 16 mm. In comparison to the pin joint, efficiency of joint with the use of washer at zero Nm torque is increased by 5%. At w/d ratio as 4 and 5, although the bearing failure mode was observed in most of the cases and the failure load found to be increased but the joint efficiency remained almost same. Therefore this result implies that ratio of slope of strength of joint to strength of laminate

becomes almost constant after w/d ratio 4. At each w/d ratio, the effect of torque is observed. Joint efficiency of torqued joint is more than that of at 0 Nm.

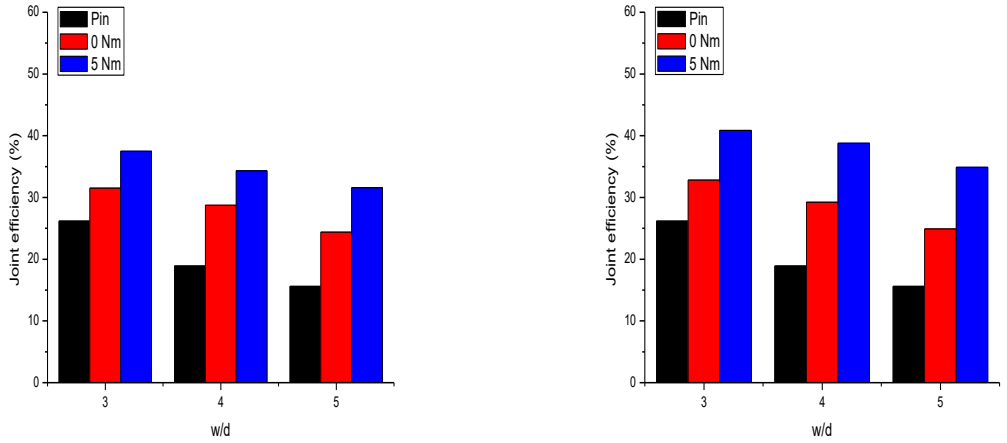

(a) (b)

Fig. 3.15 Joint efficiency at e/d = 3 (a) Washer 12 mm (b) Washer 16 mm

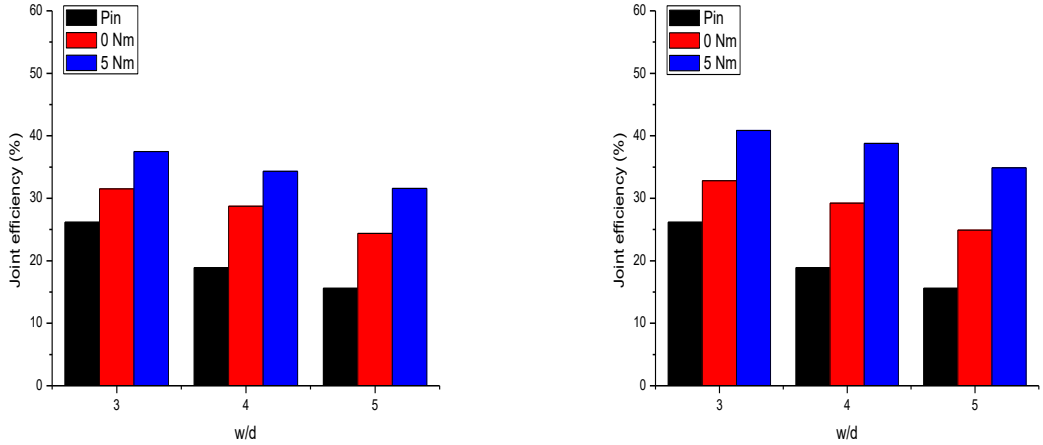

(a) (b)

Fig. 3.16 Joint efficiency at e/d = 4 (a) Washer 12 mm (b) Washer 16 mm

3.5.2 Effect of width to diameter ratio on the failure load

From fig. 3.17 and fig. 3.18 it is clear that for the edge-to-diameter ratio≥ 3, ultimate load found to be constant in the identical conditions. Therefore e/d ratio≥ 3 can be assumed as the threshold value. Whereas, ultimate load carrying capacity of specimen increases with increase in width-to-diameter ratio and bolt pretension.

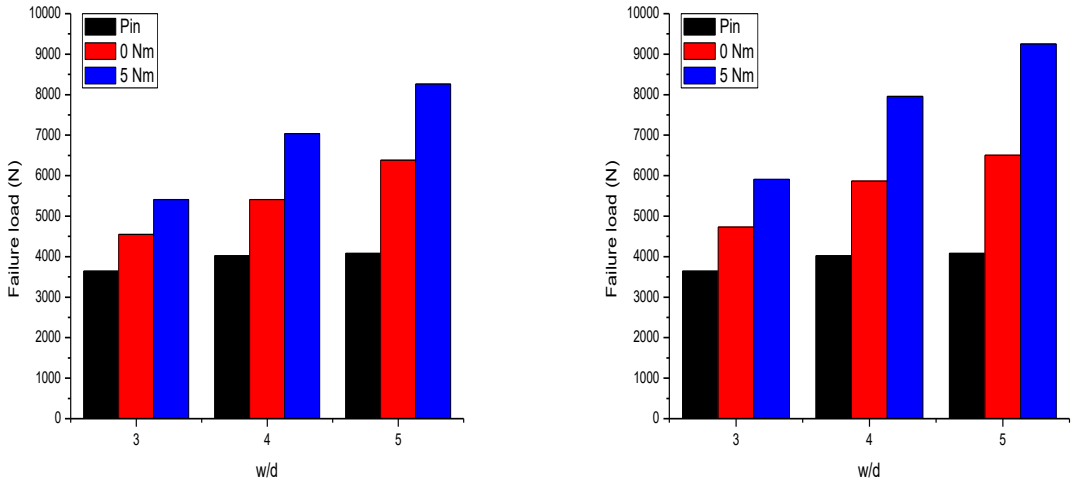

Fig. 3.17 Failure load at e/d = 3 (a) Washer 12 mm (b) Washer 16 mm

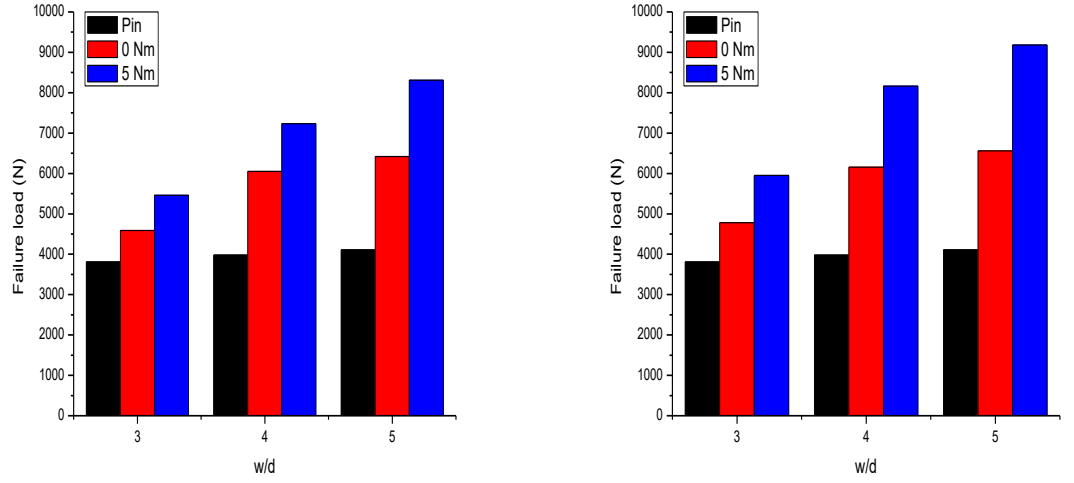

Fig. 3.18 Failure load at e/d = 4 (a) Washer 12 mm (b) Washer 16 mm

Failure load is increased up to the bearing mode of failure, no further change in ultimate failure load is observed at no preload condition of bolt joint. At w/d = 3, net-tension failure mode is observed but it changed to bearing mode of failure at w/d = 4 and 5 at finger tight condition. Corresponding to the failure mode at different w/d ratio, failure load is increased when w/d changed from w/d = 3 to 4 but no further change in failure load is observed. Failure load also varies with change in failure mode as no change in failure load is observed at 0 Nm torque when w/d changes from 4 to 5 and failure mode remained bearing.

3.5.3 Effect of torque on failure load

The effect of torque on failure load was observed at each value of w/d ratio and each type of washer. But at the higher value of w/d ratio, effect of torque is more. The effect of e/d ratio, which is related to the shear failure behaviour of joint was negligible as no shear failure behaviour was observed in single lap single bolt joint. In fig. 3.19 - 3.21, W1 and W2 are the washers of diameter of 12 mm and 16 mm respectively.

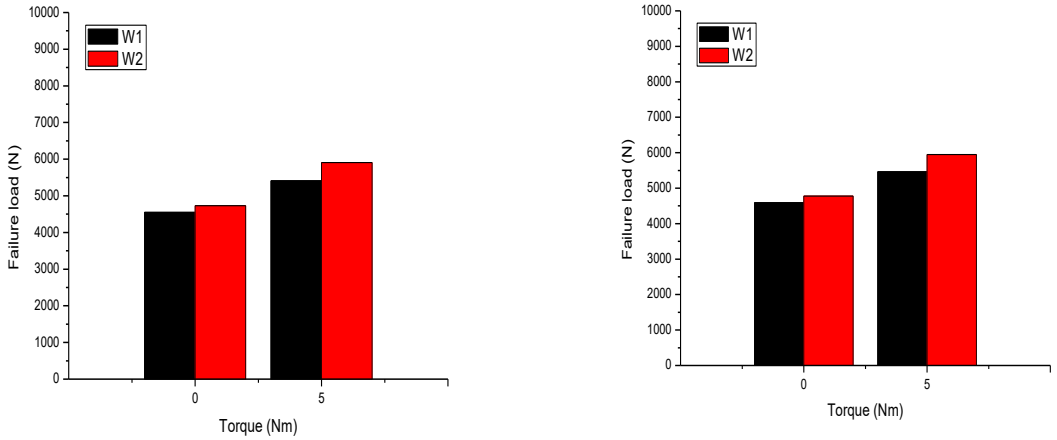

(a) (b)

Fig. 3.19 Failure load using W1 and W2 at (a) w/d = 3 and e/d = 3 (b) w/d = 3 and e/d = 4

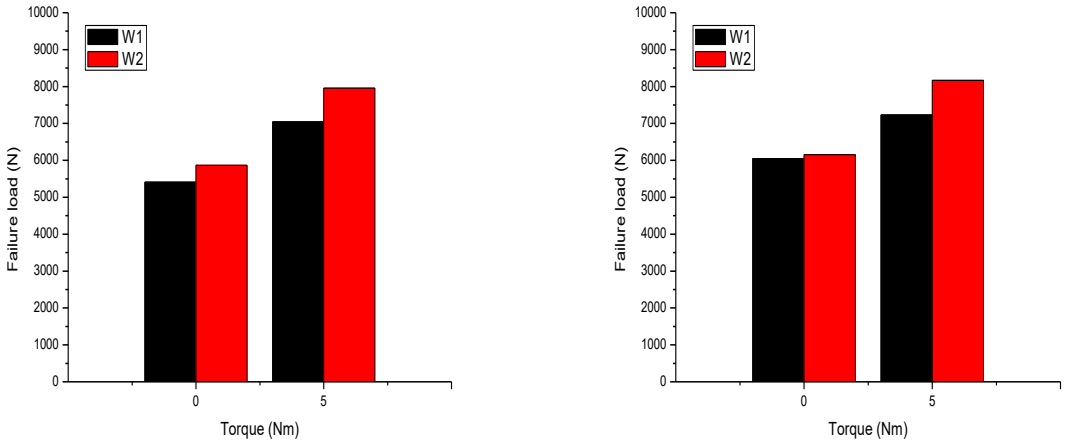

(a) (b)

Fig. 3.20 Failure load using W1 and W2 at (a) w/d = 4 and e/d = 3 (b) w/d = 4 and e/d = 4

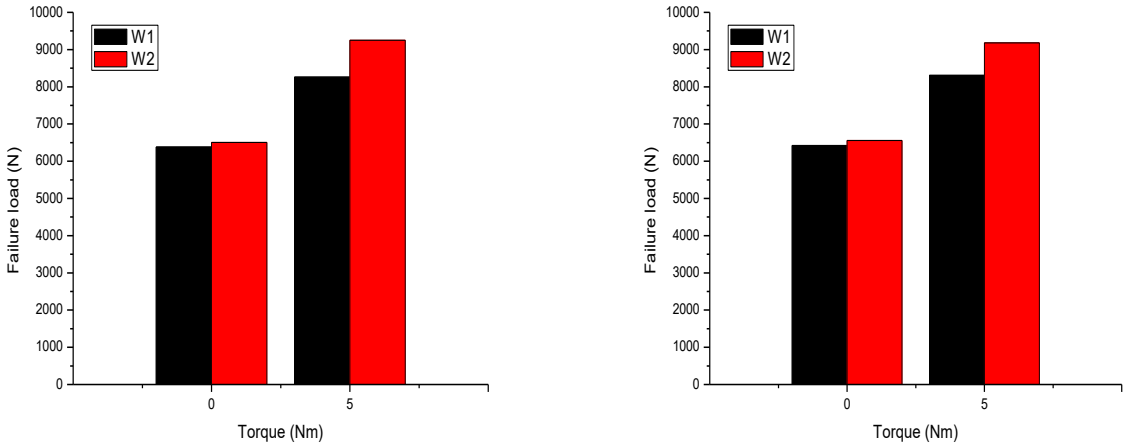

(a) (b)

Fig. 3.21 Failure load using W1 and W2 at (a) w/d = 5 and e/d = 3 (b) w/d = 5 and e/d = 4

Approximately, there was an increase of 25% failure load with increase in torque from 0 Nm to 5 Nm at the low value of w/d ratio and 42% increase at high value of w/d ratio. As the washer outer diameter increases, knee growth of damage take place which is observed in most of the load-displacement curve of specimen tested with the washer of 16 mm outer diameter. This type of damage take place due to the decrease in pressure with increase in lateral constraint area. But the ultimate failure load increases which may be due to increase in damage area and due to low degree of damage.

3.5.4 Effect of parameters on stiffness of joint

Clamping area or the restrained area increases as the outer diameter of washer increases. But effective pressure imparted by washer decreases as the outer diameter of washer increases when the testing take place under the identical conditions, the reduction in effective pressure reduces the stiffness of joint.

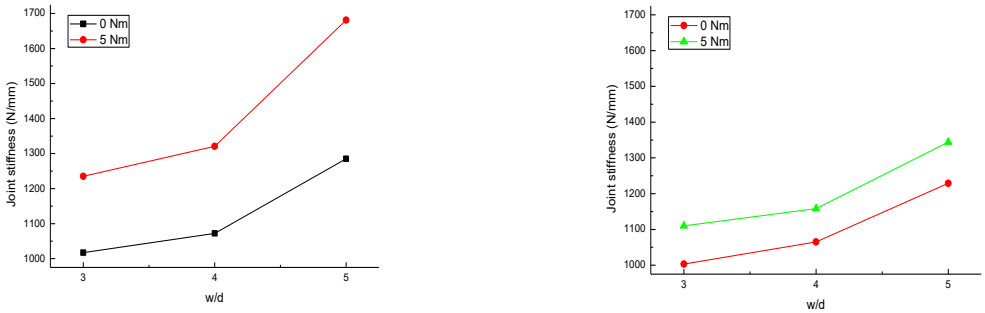

(a) (b)

Fig. 3.22 Joint stiffness at e/d = 3 (a) Washer 12 mm (b) Washer 16 mm

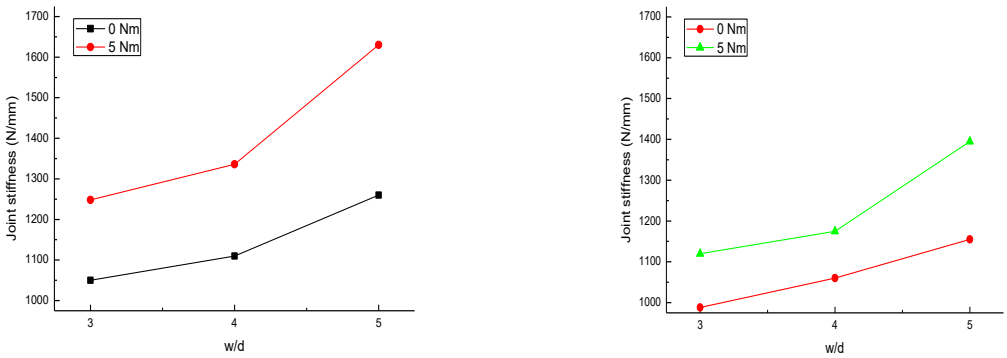

(a) (b)

Fig. 3.23 Joint stiffness at e/d = 4 (a) Washer 12 mm (b) Washer 16 mm

Fig. 3.22 and Fig. 3.23 shows approximately the same results which implies that chosen e/d ratio does not affect the joint stiffness. Whereas, w/d ratio and washer outer diameter affect joint stiffness, stiffness increases as the w/d ratio increase but decrease with increase in outer diameter of washer. As shown in the fig. 3.22 and 3.23, slope of stiffness curve is higher between w/d ratio as 4 and 5 than the slope of curve between w/d = 3 and 4.

It is clear from fig. 3.22 that the slope of curve with washer diameter 12 mm not only increases with increase in w/d ratio but also increase with increase in torque. Whereas in case of washer with diameter 16 mm slope at 5 Nm torque increases with same manner as it is increases at torque 0 Nm with respect to w/d ratio.

3.5.5 Effect of torque and washer diameter on joint stiffness

Joint stiffness and joint strength are the important factors of structural design. In this study, out of the four parameters, three parameters were found to be effective in case of joint stiffness. The pressure applied through washer can be calculated using equation (3.3) given by Park *et al.* [33].

$$\sigma_{press} = \frac{1000\,T}{(\pi/_4)kd(D^2-d^2)} \tag{3.3}$$

Where, T is applied torque (Nm), σ_{press} is bolt pretension pressure (Mpa), D is washer outer diameter (mm), d is nominal diameter of bolt (mm) and k is torque coefficient (0.2).

In fig. 3.24 – 3.26, W1 and W2 are the washers of diameter of 12 mm and 16 mm respectively.

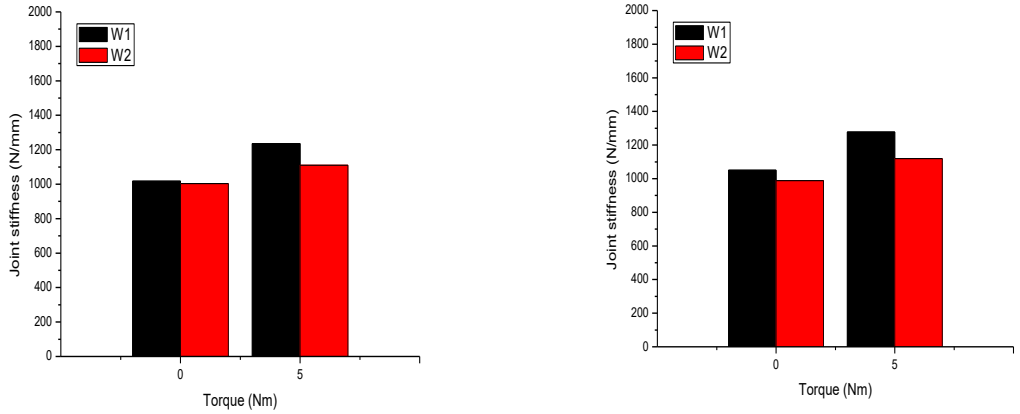

(a) (b)

Fig. 3.24 Joint stiffness using W1 and W2 at (a) w/d = 3 and e/d = 3 (b) w/d = 3 and e/d = 4

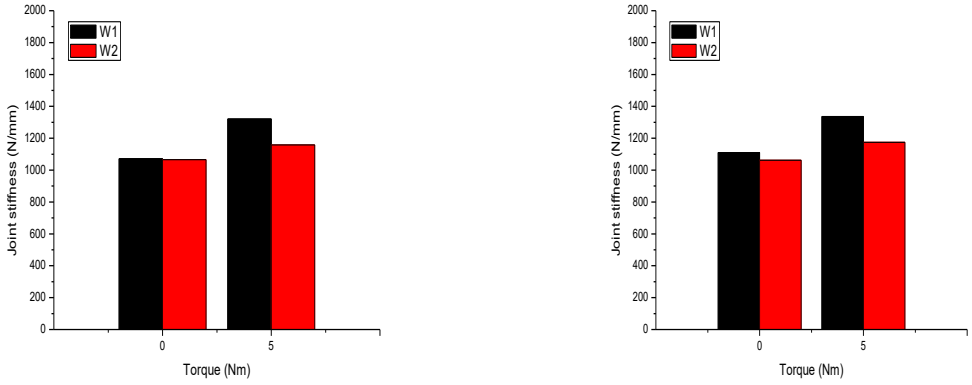

(a) (b)

Fig. 3.25 Joint stiffness using W1 and W2 at (a) w/d = 4 and e/d = 3 (b) w/d = 4 and e/d = 4

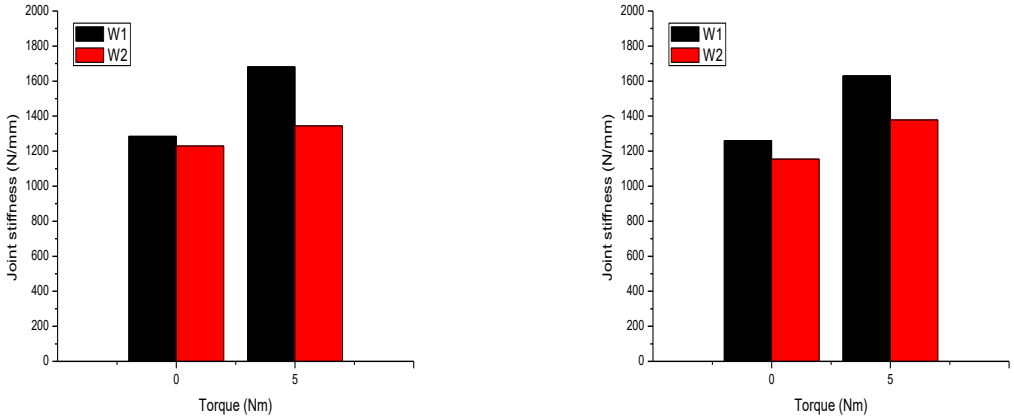

(a) (b)

Fig. 3.26 Joint stiffness using W1 and W2 at (a) w/d = 5 and e/d = 3 (b) w/d = 5 and e/d = 4

Although at the lower value of w/d ratio, use of torque and washer was not effective on the joint efficiency. But at the higher value of w/d ratio, a clear effect of washer at higher torque levels was observed. For the same value of torque, washer with the lower outer diameter depicts the higher joint stiffness. Under the identical conditions, pressure applied through the washer of lesser diameter is more and this increase in pressure in the vicinity of hole results in the increase in joint stiffness at initial phase.

Table 3.6 shows the failure load, joint stiffness and failure mode obtained from the testing of specimens of 30 groups, three samples of each group were tested as per the instructions given in the ASTM D3039-14 [29]. The average value of three samples for each group is reported. In Table 3.6, B stands for bearing mode of failure and NT is the net-tension mode of failure.

Table 3.6 Comparison of strength, stiffness and failure mode of different groups

Specimens	Failure load (N)	Stiffness (N/mm)	Failure Mode
1.	3640	909	NT
2.	4550	1017	NT
3.	4730	1003	NT
4.	5410	1235	NT
5.	5910	1110	NT
6.	4020	968	B
7.	5810	1072	B
8.	5865	1065	B
9.	7040	1321	B+NT
10.	7955	1158	B+NT
11.	4080	1050	B
12.	6380	1285	B
13.	6505	1229	B
14.	8260	1681	B
15.	9250	1344	B
16.	3810	1080	B+NT
17.	4590	1081	NT
18.	4780	1010	NT
19.	5460	1278	NT
20.	5950	1095	NT
21.	3980	1045	B
22.	6050	1110	B
23.	6155	1062	B
24.	7230	1336	B+NT
25.	8165	1175	B+NT
26.	4110	1160	B

27.	6420	1260	B
28.	6560	1155	B
29.	8310	1630	B
30.	9180	1395	B

3.5.6 Failure modes

Fig. 3.27 – 3.29 shows the actual images of specimens with different failure modes.

(a) (b)

Fig. 3.27 Failure mode at w/d = 3 (a) Torque 0 Nm (b) Torque 5 Nm

(a) (b)

Fig. 3.28 Failure mode at w/d = 4 (a) Torque 0 Nm (b) Torque 5 Nm

(a) (b)

Fig. 3.29 Failure mode at w/d = 5 (a) Torque 0 Nm (b) Torque 5 Nm

The fibre reinforced composites can fail in different failure mode such as bearing mode, net-tension mode, shear-out mode or the combination of all these. Fig. 3.27 shows that both the samples at torque 0 Nm and 5 Nm fails with the net-tension mode of failure at w/d = 3. It is clear from fig. 3.28 that the failure mode in case of figure tight condition is changed from net-tension to bearing mode of failure when w/d ratio changed from 3 to 4, whereas it remains net-tension at a torque of 5 Nm. Fig. 3.29 (b) shows that in fully clamped conditions, lateral constrained provided by washer reduced the delamination near the hole and reduced degree of damage but damage is severe but at this w/d ratio failure was bearing at a torque of 5 Nm, instead of catastrophic failure. Instead of catastrophic failure, progressive failure take place at large value of w/d ratio. In case of finger tight conditions at w/d = 5 as shown in fig. 3.29 (a), significant delamination was observed at the end distances and near the hole.

CHAPTER 4

NUMERICAL ANALYSIS

In the bolted joint, bolt hole is the region of stress concentration, where the stresses are high, but this high value of stresses does not leads to the failure of joint. Due to this stress concentration around the hole, it is difficult to calculate numerical value of the actual bearing strength of joint and the strength of joint is underestimated. So it is difficult to evaluate joint behaviour numerically. But Chang *et al.* [34] proposed a method of characteristic curve to predict failure load and failure mode of composite mechanical joint around the hole. This chapter deal with the numerical analysis of single lap joint. Commercial available software ANSYS has been used along with the Tsai-Wu failure criteria to analyse single lap, single bolt joint numerically.

4.1 Characteristic curve method

Characteristic curve is an artificial curve which is calculated numerically by the compressive and tensile characteristic lengths. The characteristic length may vary with geometry and material, but it is independent of applied load as the stress distribution is not changed, only the magnitude of stresses is changed with respect to the applied load [5]. By using this method, failure of composite joint is determined on characteristic curve instead of edge of bolt hole.

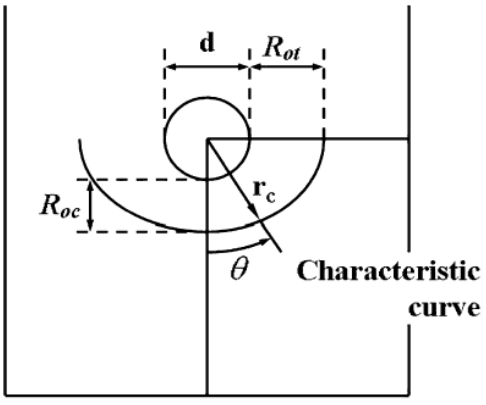

Fig. 4.1 Schematic diagram of characteristic curve [5]

The curve is drawn as shown in fig. 4.1 as per the equation 4.1 by using the characteristic lengths.

$$r_c = \frac{d}{2} + R_{ot} + (R_{oc} - R_{ot})cos\theta \quad (4.1)$$

Where, r_c is radius of characteristic curve, R_{ot} is characteristic length in tension and R_{oc} is characteristic length in compression.

Characteristic curve is symmetric to the axis of the applied load and the angle θ can be measured either clockwise or anticlockwise from the axis of applied load. To predict the failure mode Chang *et al.* [34] suggested the equation (4.2).

$0° \leq \theta \leq 15°$: Bearing failure

$30° \leq \theta \leq 60°$: Shear-out failure

$75° \leq \theta \leq 90°$: Net-tension failure (4.2)

Failure mode can be estimated on the basis of stresses on characteristic curve. Characteristic curve used along with failure theory gives the idea about the failure load and failure mode of joint.

4.2 Failure criteria

Numerically failure load can be calculated on the basis of Failure Index (FI) on characteristic curve. Tsai-Wu failure criteria [35] shown in equation (4.3) can be used to determine failure of joint.

$$F_1\sigma_1 + F_2\sigma_2 + F_{11}{\sigma_1}^2 + F_{22}{\sigma_2}^2 + F_{66}{\sigma_6}^2 + 2F_{12}\sigma_1\sigma_2 = FI \quad (4.3)$$

Where, $F_1, F_2, F_{11}, F_{22}, F_{66}$ and F_{12} are the Tsai-Wu equation polynomial and associated to the properties of laminate and later calculated experimentally. σ_1, σ_2 and σ_6 are the maximum principle stress, minimum principle stress and maximum shear stress respectively and calculated numerically.

Following equations from (4.4) to (4.9) are used to calculate Tsai-Wu polynomials.

$$F_1 = \frac{1}{X_t} - \frac{1}{X_c} \quad (4.4)$$

$$F_2 = \frac{1}{Y_t} - \frac{1}{Y_c} \quad (4.5)$$

$$F_{11} = \frac{1}{X_t X_c} \quad (4.6)$$

$$F_{22} = \frac{1}{Y_t Y_c} \quad (4.7)$$

$$F_{66} = \frac{1}{S^2} \quad (4.8)$$

$$F_{12} = -0.5\sqrt{F_{11}F_{12}} \quad (4.9)$$

Failure of joint can be estimated by using equation (4.3). Failure Index (FI) defines the failure of joint as following.

If $FI < 1$, no failure of joint

If $FI > 1$, failure of joint

Failure load of joint can be calculated numerically by using the equation (4.10).

$$F = \frac{P}{FI} \tag{4.10}$$

Where, F is failure load, P is applied load and FI is Failure Index at curve.

Failure Index can be calculated using the equation (4.3). the value of induced stresses at characteristic curve are put into the equation (4.2) to calculate Failure Index and the value of failure index on the characteristic curve defines the mode of failure of joint. Equation (4.10) which is the ratio of applied load to failure index gives safe load that the joint can carry without failure.

4.3 Finite element modelling

Static structural analysis of single lap single lap bolt joint was carried out to find out failure load and failure mode of different configurations as shown in Table 3.5. Static structure module involved three major phases *i.e.*, Pre-processing, Solver and Post-processing for the analysis purpose and are explained below.

4.3.1 Pre-Processing

In this phase material properties are assigned to the model as mentioned in Table 3.5. Geometric model was developed and finite element mesh was generated. Boundary conditions *i.e.*, applied load and supports were also applied to the model in this phase. Fig. 4.2 (a) and (b) shows the geometry and boundary conditions given to the bearing test specimen to find the compressive characteristic length and tensile test specimen to find the tensile characteristic length respectively. Analysis to form characteristic curve was carried out in Post-Processing module which is explained below. After calculating the characteristic lengths, characteristic curve was formed around the hole of the model. Developed model was sliced at different planes and the connection between sliced parts was made so that desired mesh can be formed. Frictional contact between different bodies were defined as shown in fig. 4.3. Number of elements and number of nodes for different configurations were generated as shown in Table 4.1. Fig. 4.4 (a) shows the overall view model with the quadrilateral element mesh and fig. 4.4 (b) shows the refined mesh around the bolt hole and along the characteristic curve to improve the accuracy of result. The boundary conditions given to the model are shown in the fig. 4.5. In the fixed end, displacement is set to zero in all directions as shown in fig. 4.5. The load is applied in two steps. In the first step, bolt pre-tension is applied and in the second step force (P) is applied on the other end to the fixed end. Torque applied on bolt can be converted into the preload (N) developed by the bolt on the laminate plates using the equation (4.11) discussed by Qin *et al.* [14].

$$P_L = \frac{T}{kd} \tag{4.11}$$

Where, P_L is preload (N), T is applied torque (Nm), k is torque coefficient (0.2) and d is nominal diameter of bolt (m).

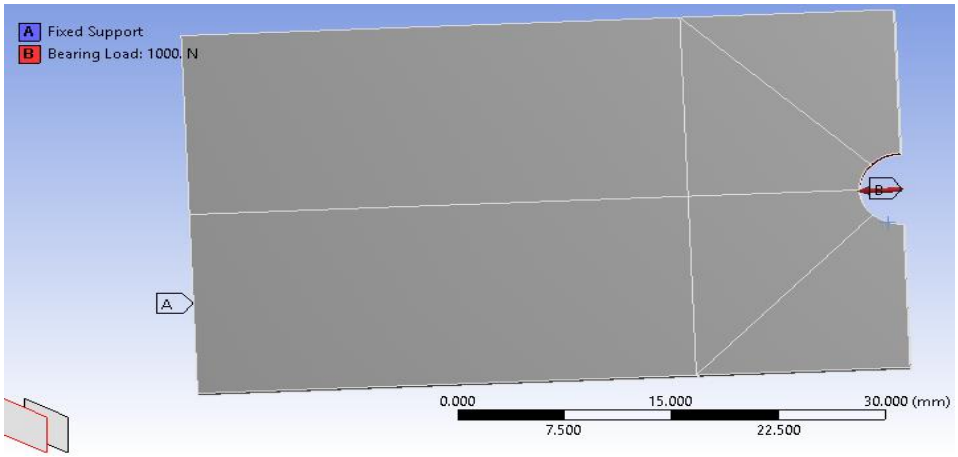

(a)

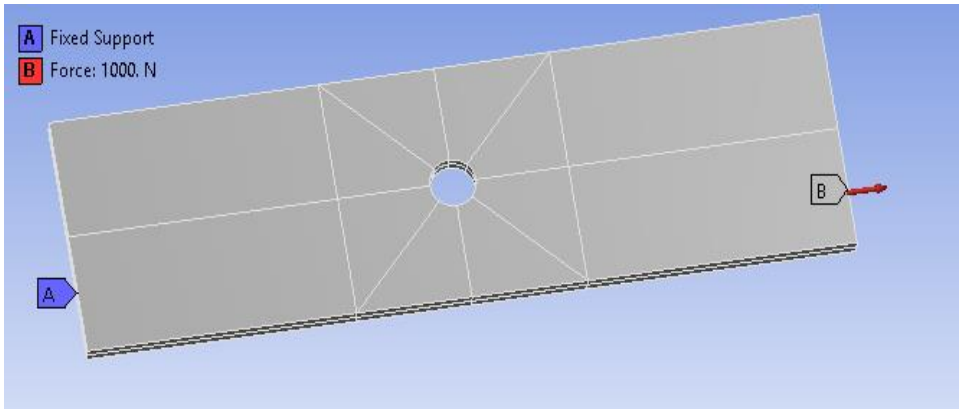

(b)

Fig. 4.2 (a) Bearing test specimen (b) Tensile test specimen

Table 4.1 Number of Elements and Nodes in different geometries

Geometry	Elements	Nodes
w/d = 3	39370	178724
w/d = 4	72310	323784
w/d = 5	109570	487332

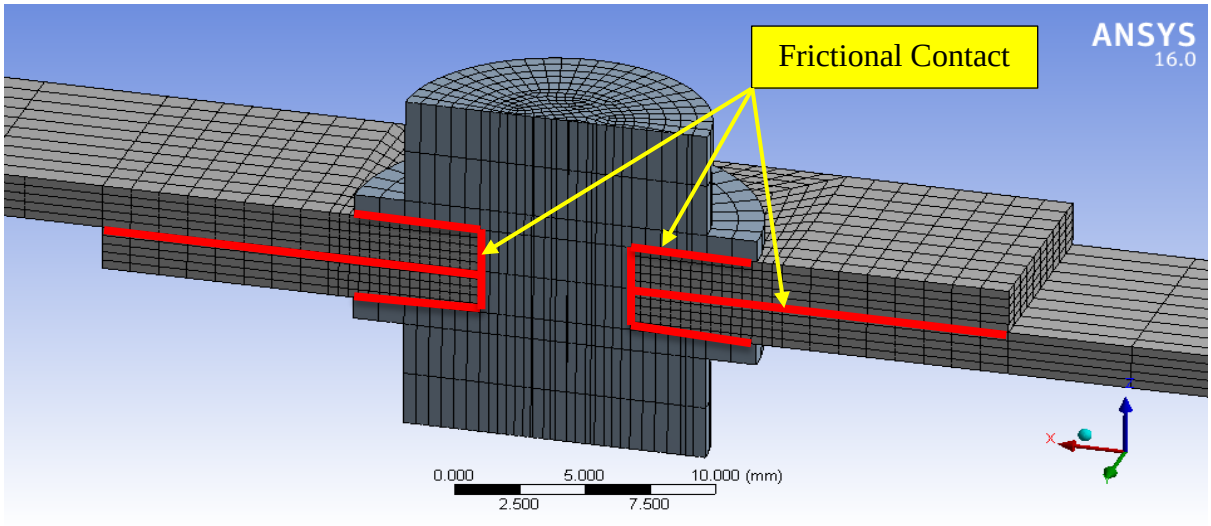

Fig. 4.3 Frictional contact between different parts

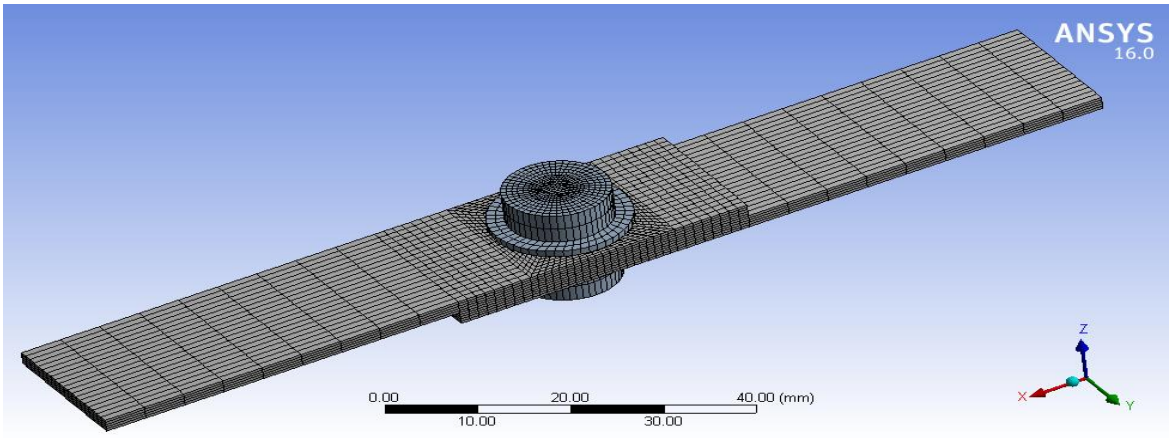

(a)

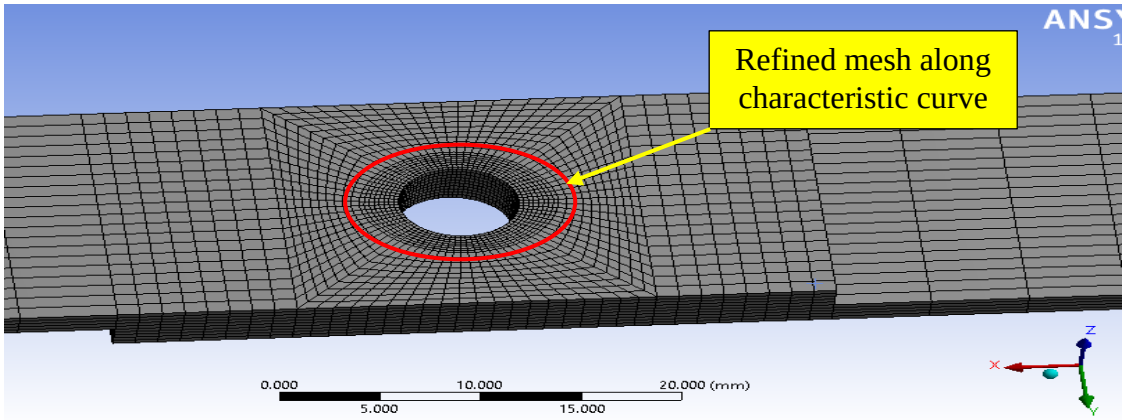

(b)

Fig. 4.4 Mesh of specimen (a) Overall mesh (b) Mesh around the hole

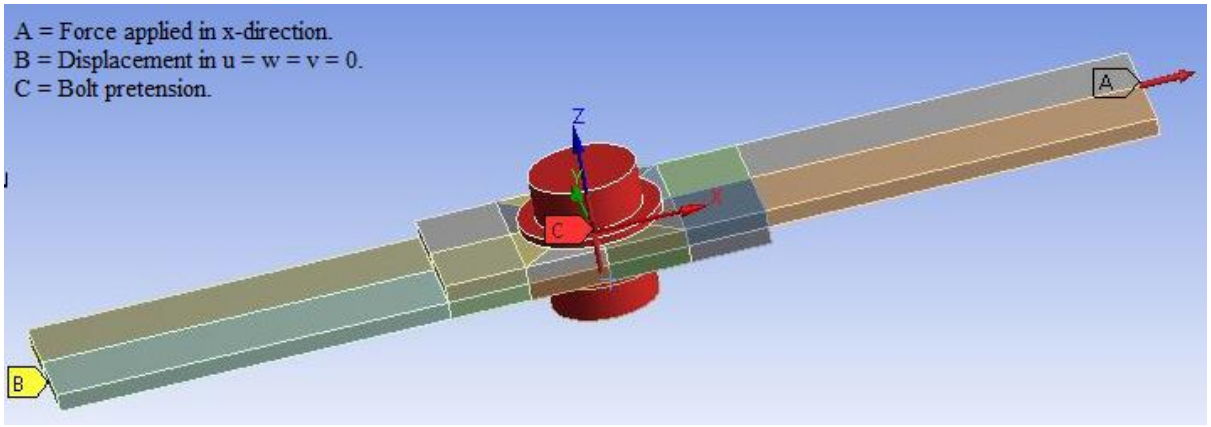

Fig. 4.5 Boundary conditions given to specimen

4.3.2 Solver

In this phase stiffness matrixes are generated and modified as the governing equations are solved. In this phase user can only see the processing of operation in the form of convergence as shown in fig. 4.6. Solution time consumption depends upon the number of elements, number of nodes and the boundary conditions. As the number of nodes increases, time taken to solve problem increases.

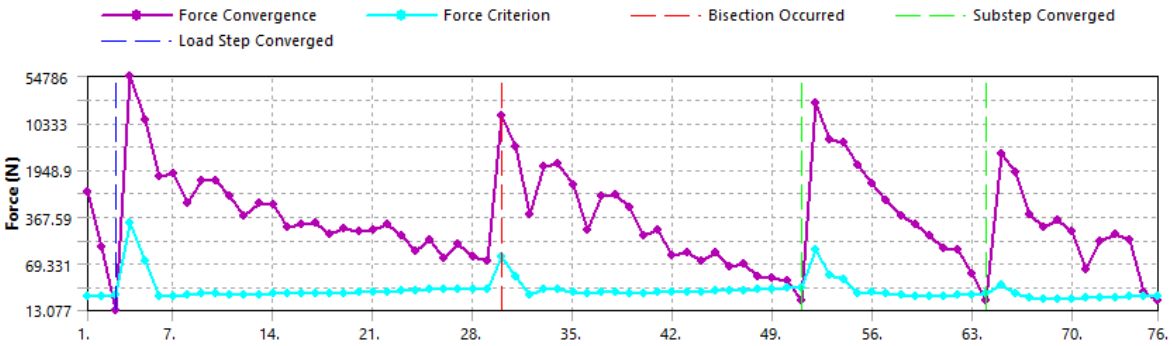

Fig. 4.6 Force convergence

4.3.3 Post-Processing

In solver geometric model has been solved under the applied boundary conditions and in the phase of post-processing of finite element method, obtained results are analyzed. Fig. 4.7 (a) and (b) shows the minimum principle stresses on bearing test specimen to calculate the compressive characteristic length (R_{oc}) and maximum principle stresses on tensile test specimen to calculate the tensile characteristic length (R_{ot}) respectively. Mean bearing strength of bearing test specimen and mean strength of tensile test specimen helps to calculate characteristic lengths and to form characteristic curve. Mean bearing strength of bearing test

specimen can be calculated using equation (4.12) and mean tensile strength of tensile test specimen can be calculated using equation (4.13).

$$\text{Mean bearing strength} = \frac{P}{d \times t} \tag{4.12}$$

$$\text{Mean tensile strength} = \frac{P}{(w-d) \times t} \tag{4.13}$$

Where, P is the applied load, w is the width of specimen, d is the diameter of hole and t is the thickness of specimen.

The point at which the maximum principle stress is equal to the mean bearing strength of the specimen, was located on the bearing test specimen as shown in fig. 4.7 (a). The distance of this point from the centre of hole is measured as R_{oc}. Similarly the point on the tensile test specimen where the value of minimum principal stress is equal to the mean tensile strength of specimen, was located. The length of this point from the centre of hole is measured as R_{ot}. These distances; $R_{ot}\ and\ R_{oc}$ are used to calculate the radius of characteristic curve r_c by using the equation (4.1). Fig. 4.8 (a), (b) and (c) shows maximum principle stresses, minimum principle stresses and maximum shear stresses respectively for the geometry of lap joint at w/d = 5 and e/d = 3. For all type of lap joint configuration, these stresses were calculated on each node of the characteristic curve. Failure Index were calculated on the nodes of the characteristic curve by using the equation (4.3), on the basis of maximum principle stresses, minimum principle stresses and maximum shear stresses on the node. Maximum magnitude of Failure Index on the node of characteristic curve defines the failure mode and failure load. Failure load was calculated using equation (4.10) by dividing maximum value of Failure Index of node to the applied load. Equation (4.2) used to calculate the failure mode, angle θ was the measured in anticlockwise direction up to a node at which Failure Index is maximum on the characteristic curve.

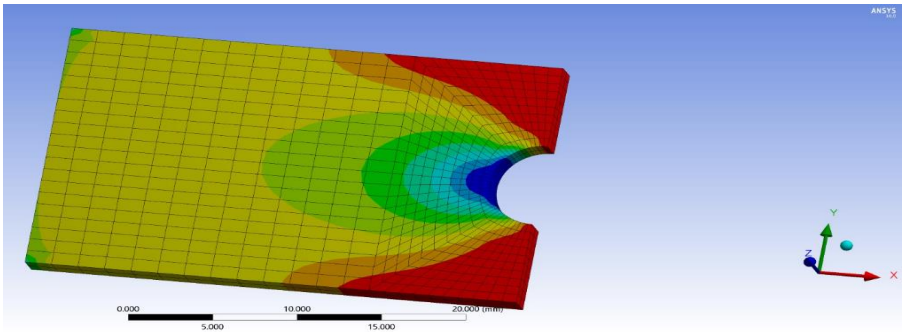

(a)

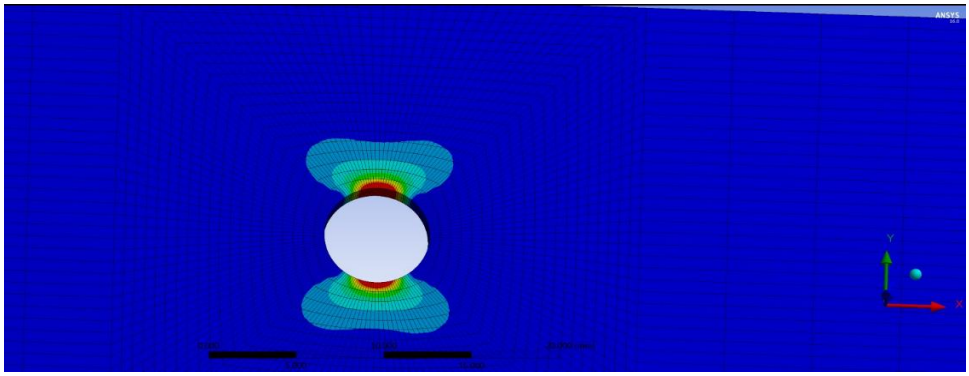

(b)

Fig. 4.7 Test specimens (a) Bearing test specimen (b) Tensile test specimen

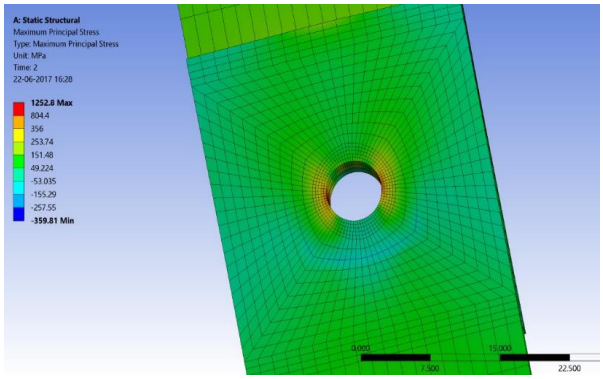

(a)

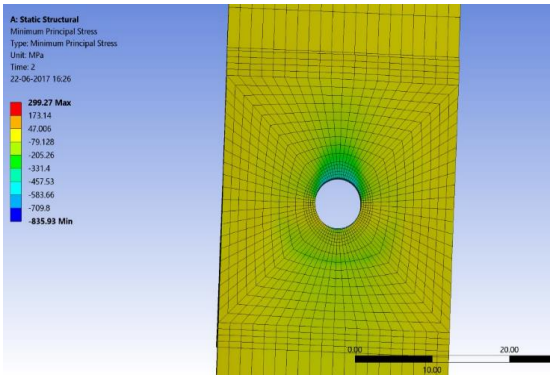

(b)

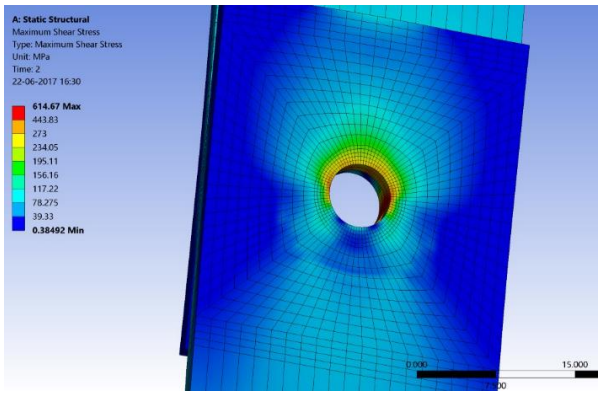

(c)

Fig. 4.8 Stresses (a) Maximum principle (b) Minimum principle (c) Maximum shear

Fig. 4.9 shows the failure angle for the joint with w/d = 5, e/d = 3 and 5 Nm torque on the washer of outer diameter 12 mm configuration on the characteristic curve. The failure angle shows the bearing failure mode in the said configuration. The failure load on characteristic curve was measured on the basis of failure index calculation of the curve nodes. Fig. 4.10

shown the secondary bending of joint in the modelling of single lap joint due the eccentricity of applied load which was also visible in experimental specimens.

Table 4.2 Comparison of Failure load and Failure mode of experimental and numerical results

Specimen	Failure load (N)		Failure Mode	
	Experimental	Numerical	Experimental	Numerical
1	3640	3235	NT	NT
2	4550	3868	NT	NT
3	4730	4021	NT	NT
4	5410	4760	NT	NT
5	5910	5378	NT	NT
6	4020	3819	B	B
7	5810	5345	B	NT
8	5865	5161	B	NT
9	7040	6124	B+NT	NT
10	7955	7005	B+NT	NT
11	4080	3916	B	B
12	6380	5805	B	B
13	6505	6049	B	B
14	8260	7351	B	B
15	9250	8047	B	B
16	3810	3581	B+NT	NT
17	4590	4131	NT	NT
18	4780	4398	NT	NT
19	5460	4914	NT	NT
20	5950	5415	NT	NT
21	3980	3781	B	B
22	6050	5566	B	B
23	6155	5601	B	B
24	7230	6362	B+NT	NT
25	8165	7186	B+NT	NT
26	4110	3945	B	B
27	6420	5778	B	B
28	6560	5904	B	B
29	8310	7396	B	B
30	9180	8170	B	B

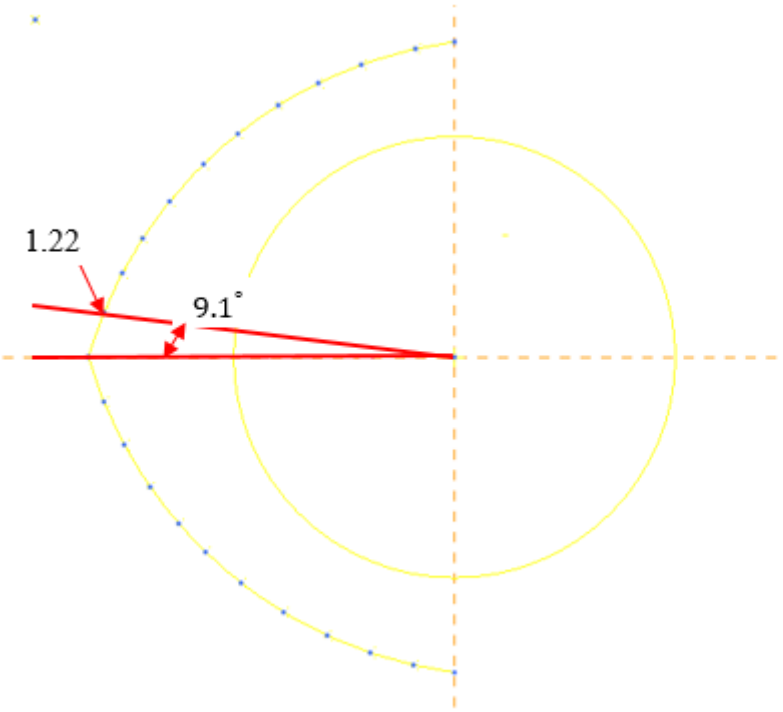

Fig. 4.9 Angle measurement of failure mode

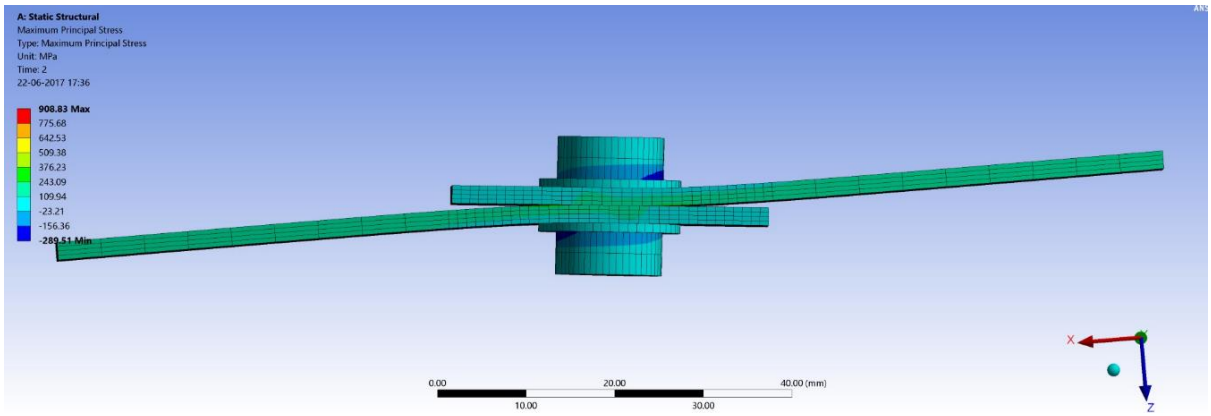

Fig. 4.10 Secondary bending of joint

The failure load and failure mode for each geometric configurations are shown in Table 4.2. It can be seen from the table that the numerical result shows a good agreement with the experimental one. In Table 4.2, B stands for bearing mode of failure and NT is the net-tension mode of failure.

CHAPTER 5
CONCLUSION

5.1 Conclusions

Woven glass fiber reinforced epoxy laminate was prepared using the hand layup technique. From the experimental as well as the numerical results of single lap single bolt joint, the following conclusions can be drawn.

(i) Failure load and the stiffness of joint is directly related to the width to diameter ratio. Increasing w/d ratio, failure load and stiffness increased. Failure load increases up to the critical value of the w/d ratio *i.e.*, w/d = 4 for 0 Nm and w/d = 5 for 5 Nm torque.

(ii) Bolt torque or preload has the significant effect on the failure load and the failure mode. For the identical conditions of 0 Nm testing at low w/d ratio, when the joint is tested at 5 Nm torque, failure load increases but failure becomes catastrophic.

(iii) Failure mode of single lap, single bolt joint changes from net-tension to bearing mode as w/d ratio increases for specimen with large e/d ratios. However, the critical value of w/d ratio changes for different torque levels.

(iv) As the outer diameter of washer decreases or the lateral constraint area decreases, which results in increase in joint stiffness but the ultimate load carrying capacity of this configuration joint is less than that of the joint with high lateral constraint area.

(v) In case of single lap joint, it can be concluded that, for e/d ratio$\geq$ 3, there is no change in the ultimate load bearing capacity and the stiffness of joint.

(vi) Although failure load increases as the w/d ratio increases but joint efficiency decreases. But the increasing trend in each w/d ratio with respect to increment in torque is observed.

(vii) For the numerical analysis of joint, characteristic curve method along with Tsai-Wu failure theory gave good correlation with the experimental results.

5.2 Future scope

The present idea of work can also be implemented into the following directions.

(i) The work can be studied on the double lap joint.

(ii) The work can be extended for the muti-bolt single lap joint.

(iii) Failure analysis of joint can be carried out under the hygrothermal conditions.

References

[1] E.J. Barbero, “Introduction to composite materials design”, 2nd ed. US: CRC press, 2010.

[2] Faruk Sen, Murat Pakdil, Onur Sayman, Semih Benli, “Experimental failure analysis of mechanically fastened joints with clearance in composite laminates under preload”, Materials and Design 29 (2008) 1159–1169.

[3] U.A. Khashaba, H.E.M. Sallam, A.E. Al-Shorbagy, M.A. Seif, “Effect of washer size and tightening torque on the performance of bolted joints in composite structures”, Composite Structures 73 (2006) 310–317.

[4] M.A. McCarthy, V.P. Lawlor, W.F. Stanley, C.T. McCarthy, “Bolt-hole clearance effects and strength criteria in single-bolt, single-lap, composite bolted joints”, Composites Science and Technology 62 (2002) 1415–1431.

[5] Jin-Hwe Kweon, Hyon-Su Ahn, Jin-Ho Choi, “A new method to determine the characteristic lengths of composite joints without testing”, Composite Structures 66 (2004) 305–315.

[6] Yi Xiao, Takashi Ishikawa, “Bearing strength and failure behavior of bolted composite joints (part I: Experimental investigation)”, Composites Science and Technology 65 (2005) 1022–1031.

[7] Yi Xiao, Takashi Ishikawa, “Bearing strength and failure behavior of bolted composite joints (part II: modeling and simulation)”, Composites Science and Technology 65 (2005) 1032–1043.

[8] Gordon Kelly, “Load transfer in hybrid (bonded/bolted) composite single-lap joints”, Composite Structures 69 (2005) 35–43.

[9] Ling Liu, Bo-Ming Zhang, Dian-Fu Wang, Zhan-Jun Wu, “Effects of cure cycles on void content and mechanical properties of composite laminates”, Composite Structures 73 (2006) 303–309.

[10] Sayed A. Nassar, Vinayshankar L. Virupaksha, Saravanan Ganeshmurthy, “Effect of Bolt Tightness on the Behavior of Composite Joints”, Journal of Pressure Vessel Technology 129 (2007) 43-51.

[11] Osman Asi, “Effect of different woven linear densities on the bearing strength behaviour of glass fiber reinforced epoxy composites pinned joints”, Composite Structures 90 (2009) 43–52.

[12] F.-X. Irisarri, F. Laurin, N. Carrere, J.-F. Maire, “Progressive damage and failure of mechanically fastened joints in CFRP laminates – Part I: Refined Finite Element modelling of single-fastener joints”, Composite Structures 94 (2012) 2269–2277.

[13] B. Egan, C.T. McCarthy, M.A. McCarthy, R.M. Frizzell, “Stress analysis of single-bolt, single-lap, countersunk composite joints with variable bolt-hole clearance”, Composite Structures 94 (2012) 1038–1051.

[14] Tianliang Qin, Libin Zhao, Jianyu Zhang, “Fastener effects on mechanical behaviors of double-lap composite joints”, Composite Structures 100 (2013) 413–423.

[15] P.J. Gray, R.M. O’Higgins, C.T. McCarthy, “Effects of laminate thickness, tapering and missing fasteners on the mechanical behaviour of single-lap, multi-bolt, countersunk composite joints”, Composite Structures 107 (2014) 219–230.

[16] Yunong Zhai, Dongsheng Li, Xiaoqiang Li, Liang Wang, Yu Yin, “An experimental study on the effect of bolt-hole clearance and bolt torque on single-lap, countersunk composite joints”, Composite Structures 127 (2015) 411–419.

[17] Manjeet Sekhon, J.S. Saini, Gaurav Singla, H. Bhunia, “Influence of nanoparticle fillers content on the bearing strength behavior of glass fiber-reinforced epoxy composites pin joints”, Journal of Materials: Design and Applications (2015) 1–16 (in press).

[18] Valbona Mara, Reza Haghani, Mohammad Al-Emrani, “Improving the performance of bolted joints in composite structures using metal inserts”, Journal of Composite Materials (2015) 1–18 (in press).

[19] Manjeet Singh, J.S. Saini, H. Bhunia, Paramdeep Singh, “Application of Taguchi method in the optimization of geometric parameters for double pin joint configurations made from glass–epoxy nanoclay laminates”, Journal of Composite Materials (2016) 1–18 (in press).

[20] Mingxia Yao, Deju Zhu, Yiming Yao, Huaian Zhang, Barzin Mobasher, “Experimental study on basalt FRP/steel single-lap joints under different loading rates and temperatures”, Composite Structures 145 (2016) 68–79.

[21] Saud Aldajah, Ghydaa Alawsi, Safaa Abdul Rahmaan, “Impact of sea and tap water exposure on the durability of GFRP laminates”, Materials and Design 30 (2009) 1835–1840.

[22] Ghydaa Alawsi, Saud Aldajah, Safa Abdul Rahmaan, “Impact of humidity on the durability of E-glass/polymer composites”, Materials and Design 30 (2009) 2506–2512.

[23] Abdel-Hamid I. Mourad, Beckry Mohamed Abdel-Magid, Tamer El-Maaddawy, Maryam E. Grami, “Effect of Seawater and Warm Environment on Glass/Epoxy and Glass/Polyurethane Composites”, Appl Compos Mater (2010) 17:557–573.

[24] Ibrahim Fadil Soykok, Onur Sayman, Ahmet Pasinli, “Effects of hot water aging on failure behavior of mechanically fastened glass fiber/epoxy composite joints”, Composites: Part B 54 (2013) 59–70.

[25] Ibrahim Fadil Soykok, Onur Sayman, Mustafa Ozen, Behiye Korkmaz, “Failure analysis of mechanically fastened glass fiber/epoxy composite joints under thermal effects”, Composites: Part B 45 (2013) 192–199.

[26] S. Larbi, R. Bensaada, A. Bilek, S. Djebali, “Hygrothermal ageing effect on mechanical properties of FRP laminates”, AIP Conf. Proc. 1653, 020066-1–020066-7; doi: 10.1063/1.4914257.

[27] R.M. Jones, “Mechanics of composite materials”, 2nd ed. US: Taylor & Francis, 1999.

[28] “ASTM D2584. Standard Test Method for Ignition Loss of Cured Reinforced Resins”, American Society for Testing of Materials, 2000.

[29] “ASTM D3039. Standard test method for tensile properties of polymer matrix composite materials”, American Society for Testing of Materials, 2014.

[30] “ASTM D790. Standard test methods for flexural properties of unreinforced and reinforced plastics and electrical insulating materials”, American Society for Testing of Materials, 2010.

[31] P. Camanho, S.R. Hallett, “Composite joints and connections: principles, modelling and testing”, UK: Woodhead Publishing, 2011.

[32] V.B. Bhandari, “Design of machine elements. 2010”, 3rd ed. New Delhi: Tata McGraw-Hill Education, 2010.

[33] Heung-Joon Park, “Effect of stacking sequence and clamping force on the bearing strengths of mechanically fastened joints in composite laminates”, Composite Structures 53 (2001) 213-221.

[34] Fu-Kuo Chang, Richard A. Scott, George S. Springer, “Strength of Mechanically Fastened Composite Joints”, Journal of Composite Materials 1982 16: 470.

[35] Stephen W. Tsai, Edward M. Wu, “A General Theory of Strength for Anisotropic Materials”, Journal of Composite Materials 1971 5: 58.

[36] W. Van Paepegem, J. Degrieck, “Calculation of damage-dependent directional failure indices from the Tsai–Wu static failure criterion”, Composites Science and Technology 63 (2003) 305–310.

[37] Ramazan Karakuzu, Cihan Rıza¸ Calıskan, Mehmet Aktas, Bulent Murat Icten, “Failure behavior of laminated composite plates with two serial pin-loaded holes”, Composite Structures 82 (2008) 225–234.

[38] R.M. O’Higgins, M.A. McCarthy, C.T. McCarthy, “Comparison of open hole tension characteristics of high strength glass and carbon fibre-reinforced composite materials”, Composites Science and Technology 68 (2008) 2770–2778.

[39] Onur Sayman, Ramazan Siyahkoc, Faruk Sen, Resat Ozcan, “Experimental Determination of Bearing Strength in Fiber Reinforced Laminated Composite Bolted Joints under Preload”, Journal of Reinforced Plastics and Composites 2007 26: 1051.